

Voltammetry

Voltammetry comprises a group of electroanalytical methods in which information about the analyte is obtained by measuring current as a function of applied potential under conditions that promote polarization of an indicator, or working, electrode. When current proportional to analyte concentration is monitored at fixed potential, the technique is called **amperometry**. Generally, to enhance polarization, working electrodes in voltammetry and amperometry have surface areas of a few square millimeters at the most and, in some applications, a few square micrometers or less.



Throughout this chapter, this logo indicates an opportunity for online self-study at www.thomsonedu.com/chemistry/skoog, linking you to interactive tutorials, simulations, and exercises.

Let us begin by pointing out the basic differences between voltammetry and the two types of electrochemical methods that we discussed in earlier chapters. Voltammetry is based on the measurement of the current that develops in an electrochemical cell under conditions where concentration polarization exists. Recall from Section 22E-2 that a polarized electrode is one to which we have applied a voltage in excess of that predicted by the Nernst equation to cause oxidation or reduction to occur. In contrast, potentiometric measurements are made at currents that approach zero and where polarization is absent. Voltammetry differs from coulometry in that, with coulometry, measures are taken to minimize or compensate for the effects of concentration polarization. Furthermore, in voltammetry there is minimal consumption of analyte, whereas in coulometry essentially all of the analyte is converted to another state.

Voltammetry is widely used by inorganic, physical, and biological chemists for nonanalytical purposes, including fundamental studies of oxidation and reduction processes in various media, adsorption processes on surfaces, and electron-transfer mechanisms at chemically modified electrode surfaces.

Historically, the field of voltammetry developed from *polarography*, which is a particular type of voltammetry that was invented by the Czechoslovakian chemist Jaroslav Heyrovsky in the early 1920s.¹ Polarography differs from other types of voltammetry in that the working electrode is the unique *dropping mercury electrode*. At one time, polarography was an important tool used by chemists for the determination of inorganic ions and certain organic species in aqueous solutions. In the late 1950s and the early 1960s, however, many of these analytical applications were replaced by various spectroscopic methods, and polarography became a less important method of analysis except for certain special applications, such as the determination of molecular oxygen in solutions. In the mid-1960s, several major modifications of classical voltammetric techniques were developed that enhanced significantly the sensitivity and selectivity of the method. At about this same time, the advent of low-cost operational amplifiers made possible the commercial development of relatively inexpensive instruments that incorporated many of these modifications and made them available to all chemists. The result was a resurgence of interest in

¹J. Heyrovsky, *Chem. Listy*, **1922**, *16*, 256. Heyrovsky was awarded the 1959 Nobel Prize in Chemistry for his discovery and development of polarography.

Name

(a) Linear scan

(c) Square wave

applying
of a ho
ceutical.
the inve
papers l
Research
troanaly
peaked
1973. Si
ods has
of grow
2005 on
This de
the use
well as
nature
of fast
metho
phy or
source
Alt!
voltarr

²A. Bon
tion of V
C. M. A
istry, A.
Electrou
pp. 105-
ed., Nev
in *Elect*
man, ed

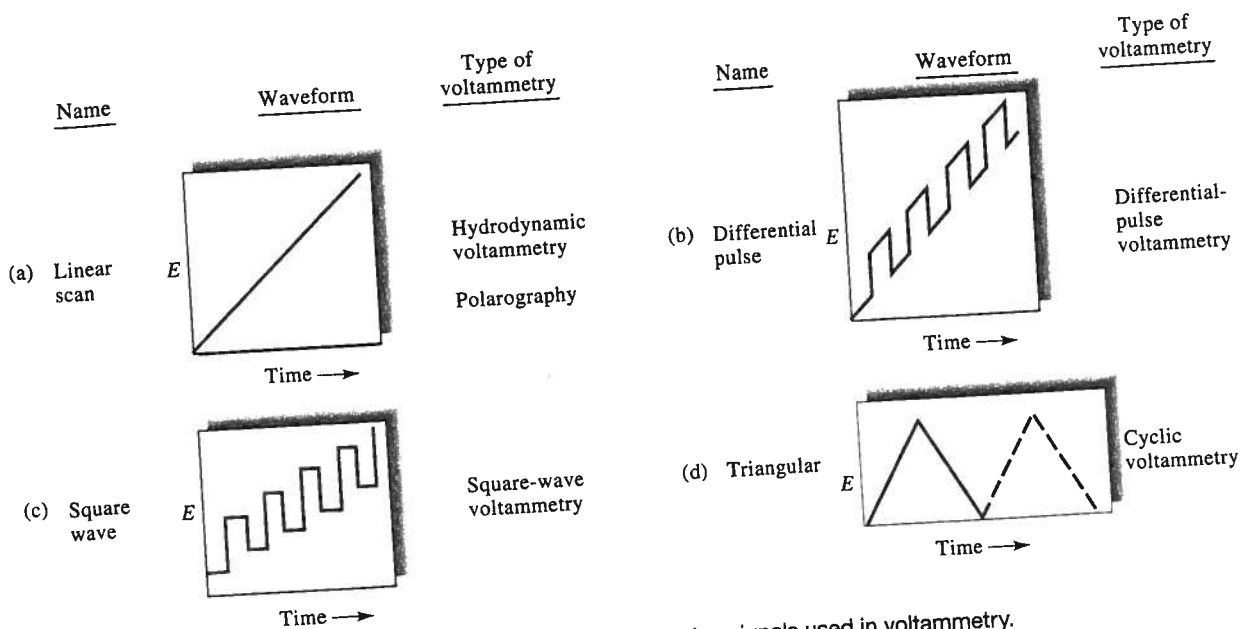


FIGURE 25-1 Voltage versus time excitation signals used in voltammetry.

applying polarographic methods to the determination of a host of species, particularly those of pharmaceutical, environmental, and biological interest.² Since the invention of polarography, at least 60,000 research papers have appeared in the literature on the subject. Research activity in this field, which dominated electroanalytical chemistry for more than five decades, peaked with nearly 2,000 published journal articles in 1973. Since that time, interest in polarographic methods has steadily declined, at a rate nearly twice the rate of growth of the general chemical literature, until in 2005 only about 300 papers on these methods appeared. This decline has been largely a result of concerns about the use of large amounts of mercury in the laboratory as well as in the environment, the somewhat cumbersome nature of the apparatus, and the broad availability of faster and more convenient (mainly spectroscopic) methods. For these reasons, we will discuss polarography only briefly and, instead, refer you to the many sources that are available on the subject.³

Although polarography declined in importance, voltammetry and amperometry at working electrodes

other than the dropping mercury electrode have grown at an astonishing pace.⁴ Furthermore, voltammetry and amperometry coupled with liquid chromatography have become powerful tools for the analysis of complex mixtures. Modern voltammetry also continues to be an excellent tool in diverse areas of chemistry, biochemistry, materials science and engineering, and the environmental sciences for studying oxidation, reduction, and adsorption processes.⁵

25A EXCITATION SIGNALS IN VOLTAMMETRY

In voltammetry, a variable potential excitation signal is impressed on a working electrode in an electrochemical cell. This excitation signal produces a characteristic current response, which is the measurable quantity in this method. The waveforms of four of the most common excitation signals used in voltammetry are shown in Figure 25-1. The classical voltammetric excitation

²A. Bond, *Broadening Electrochemical Horizons: Principles and Illustration of Voltammetric and Related Techniques*, New York: Oxford, 2003; C. M. A. Brett and A. M. Oliveira Brett, in *Encyclopedia of Electrochemistry*, A. J. Bard and M. Stratmann, eds., Vol. 3, *Instrumentation and Electroanalytical Chemistry*, P. Unwin, ed., New York: Wiley, 2002, 105–24.³A. J. Bard and L. R. Faulkner, *Electrochemical Methods*, 2nd ed., New York: Wiley, 2001, Chap. 7, pp. 261–304; *Laboratory Techniques in Electroanalytical Chemistry*, 2nd ed., P. T. Kissinger and W. R. Heinemann, eds., New York: Dekker, 1996, pp. 444–61.

⁴From 1973 to 2005, the annual number of journal articles on voltammetry and amperometry grew at three times and two and one-half times, respectively, the rate of production of articles in all of chemistry.
⁵Some general references on voltammetry include A. J. Bard and L. R. Faulkner, *Electrochemical Methods*, 2nd ed., New York: Wiley, 2001; S. P. Kouyaves, in *Handbook of Instrumental Techniques for Analytical Chemistry*, Frank A. Settle, ed., Upper Saddle River, NJ: Prentice-Hall, 1997, pp. 711–28; *Laboratory Techniques in Electroanalytical Chemistry*, 2nd ed., P. T. Kissinger and W. R. Heinemann, eds., New York: Dekker, 1996; *Analytical Voltammetry*, M. R. Smyth and F. G. Vos, eds., New York: Elsevier, 1992.

signal is the linear scan shown in Figure 25-1a, in which the voltage applied to the cell increases linearly (usually over a 2- to 3-V range) as a function of time. The current in the cell is then recorded as a function of time, and thus as a function of the applied voltage. In amperometry, current is recorded at fixed applied voltage.

Two pulse excitation signals are shown in Figure 25-1b and c. Currents are measured at various times during the lifetime of these pulses. With the triangular waveform shown in Figure 25-1d, the potential is cycled between two values, first increasing linearly to a maximum and then decreasing linearly with the same slope to its original value. This process may be repeated numerous times as the current is recorded as a function of time. A complete cycle may take 100 or more seconds or be completed in less than 1 second.

To the right of each of the waveforms of Figure 25-1 is listed the types of voltammetry that use the various excitation signals. We discuss these techniques in the sections that follow.

25B VOLTAMMETRIC INSTRUMENTATION


Figure 25-2 is a schematic showing the components of a modern operational amplifier potentiostat (see Section 24C-1) for carrying out linear-scan voltammetric measurements. The cell is made up of three electrodes immersed in a solution containing the analyte and also an excess of a nonreactive electrolyte called a *supporting electrolyte*. One of the three electrodes is the work-

ing electrode, whose potential is varied linearly with time. Its dimensions are kept small to enhance its tendency to become polarized (see Section 22E-2). The second electrode is a reference electrode (commonly a saturated calomel or a silver-silver chloride electrode) whose potential remains constant throughout the experiment. The third electrode is a counter electrode, which is often a coil of platinum wire that simply conducts electricity from the signal source through the solution to the working electrode.

The signal source is a linear-scan voltage generator similar to the integration circuit shown in Figure 3-16c. The output from this type of source is described by Equation 3-22. Thus, for a constant dc input potential of E_i , the output potential E_o is given by

$$E_o = -\frac{E_i}{R_i C_f} \int_0^t dt = -\frac{E_i t}{R_i C_f} \quad (25-1)$$

The output signal from the source is fed into a potentiostatic circuit similar to that shown in Figure 25-2 (see also Figure 24-6c). The electrical resistance of the control circuit containing the reference electrode is so large ($>10^{11} \Omega$) that it draws essentially no current. Thus, the entire current from the source is carried from the counter electrode to the working electrode. Furthermore, the control circuit adjusts this current so that the potential difference between the working electrode and the reference electrode is identical to the output voltage from the linear voltage generator. The resulting current, which is directly proportional to the potential difference between the working electrode-reference

 **Tutorial:** Learn more about **voltammetric instrumentation and waveforms.**

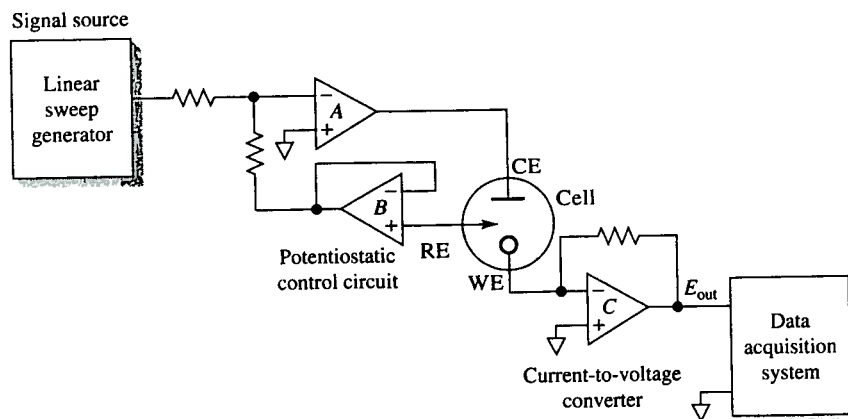


FIGURE 25-2 An operational amplifier potentiostat. The three-electrode cell has a working electrode (WE), reference electrode (RE), and a counter electrode (CE).

electro
corded
system.
dent va
workin
not the
the col
tual cc
experi

25B-

The w
variet
disks
an ine
bedde
ducto
a carl
pyrol
nano
ide; c
in Fig
with
depe
comj
Gen
by th
of th
limi
hydi
tials
of th

Ear
than
elect
or a
an e
fere
elec
com
ply
secc
this
as t
all
M
me
wit
We
era
uni

electrode pair, is then converted to a voltage and recorded as a function of time by the data-acquisition system.⁶ It is important to emphasize that the independent variable in this experiment is the potential of the working electrode versus the reference electrode and not the potential between the working electrode and the counter electrode. The working electrode is at virtual common potential throughout the course of the experiment (see Section 3B-3).

25B-1 Working Electrodes

The working electrodes used in voltammetry take a variety of shapes and forms.⁷ Often, they are small flat disks of a conductor that are press fitted into a rod of an inert material, such as Teflon or Kel-F, that has embedded in it a wire contact (see Figure 25-3a). The conductor may be a noble metal, such as platinum or gold; a carbon material, such as carbon paste, carbon fiber, pyrolytic graphite, glassy carbon, diamond, or carbon nanotubes; a semiconductor, such as tin or indium oxide; or a metal coated with a film of mercury. As shown in Figure 25-4, the range of potentials that can be used with these electrodes in aqueous solutions varies and depends not only on electrode material but also on the composition of the solution in which it is immersed. Generally, the positive potential limitations are caused by the large currents that develop because of oxidation of the water to give molecular oxygen. The negative limits arise from the reduction of water to produce hydrogen. Note that relatively large negative potentials can be tolerated with mercury electrodes because of the high overvoltage of hydrogen on this metal.

⁶Early voltammetry was performed with a two-electrode system rather than the three-electrode system shown in Figure 25-2. With a two-electrode system, the second electrode is either a large metal electrode or a reference electrode large enough to prevent its polarization during an experiment. This second electrode combines the functions of the reference electrode and the counter electrode in Figure 25-2. In the two-electrode system, we assume that the potential of this second electrode is constant throughout a scan so that the working electrode potential is simply the difference between the applied potential and the potential of the second electrode. With solutions of high electrical resistance, however, this assumption is not valid because the IR drop is significant and increases as the current increases. Distorted voltammograms are the result. Almost all voltammetry is now performed with three-electrode systems.

⁷Many of the working electrodes that we describe in this chapter have dimensions in the millimeter range. There is now intense interest in studies with electrodes having dimensions in the micrometer range and smaller. We will term such electrodes *microelectrodes*. Such electrodes have several advantages over classical working electrodes. We describe some of the unique characteristics of microelectrodes in Section 25I.

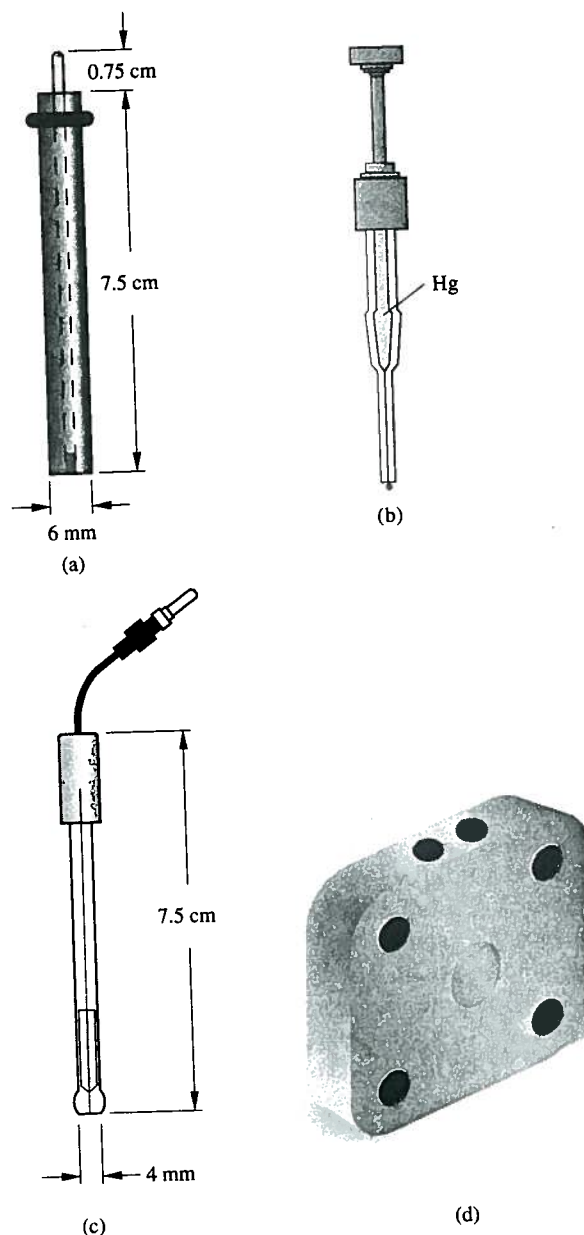
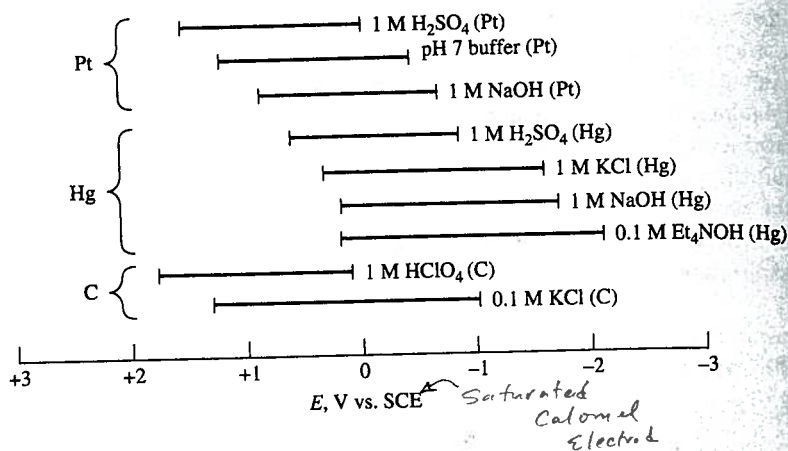


FIGURE 25-3 Some common types of commercial voltammetric electrodes: (a) a disk electrode; (b) a hanging mercury drop electrode (HMDE); (c) a microelectrode; (d) a sandwich-type flow electrode. (Electrodes [a], [c], and [d] courtesy of Bioanalytical Systems, Inc., West Lafayette, IN, with permission.)

Mercury working electrodes have been widely used in voltammetry for several reasons. One is the relatively large negative potential range just described.

FIGURE 25-4 Potential ranges for three types of electrodes in various supporting electrolytes. (Adapted from A. J. Bard and L. R. Faulkner, *Electrochemical Methods*, 2nd ed., back cover, New York: Wiley, 2001. Reprinted by permission of John Wiley & Sons, Inc.)



Furthermore, a fresh metallic surface is readily formed by simply producing a new drop. The ability to obtain a fresh surface readily is important because the currents measured in voltammetry are quite sensitive to cleanliness and freedom from irregularities. An additional advantage of mercury electrodes is that many metal ions are reversibly reduced to amalgams at the surface of a mercury electrode, which simplifies the chemistry. Mercury electrodes take several forms. **The simplest of these is a mercury film electrode formed by electrodeposition of the metal onto a disk electrode, such as that shown in Figure 25-3a.** Figure 25-3b illustrates a hanging mercury drop electrode (HMDE). The electrode, which is available from commercial sources, consists of a very fine capillary tube connected to a mercury-containing reservoir. The metal is forced out of the capillary by a piston arrangement driven by a micrometer screw. The micrometer permits formation of drops having surface areas that are reproducible to 5% or better.

Figure 25-3c shows a typical commercial microelectrode. Such electrodes consist of small-diameter metal wires or fibers (5–100 μm) sealed within tempered glass bodies. The flattened end of the microelectrode is polished to a mirror finish, which can be maintained using alumina or diamond polish or both. The electrical connection is a 0.060 in. gold-plated pin. **Microelectrodes are available in a variety of materials, including carbon fiber, platinum, gold, and silver.** Other materials can be incorporated into microelectrodes if they are available as a wire or a fiber and form a good seal with epoxy. The electrode shown is approximately 7.5 cm long and has a 4-mm outside diameter.

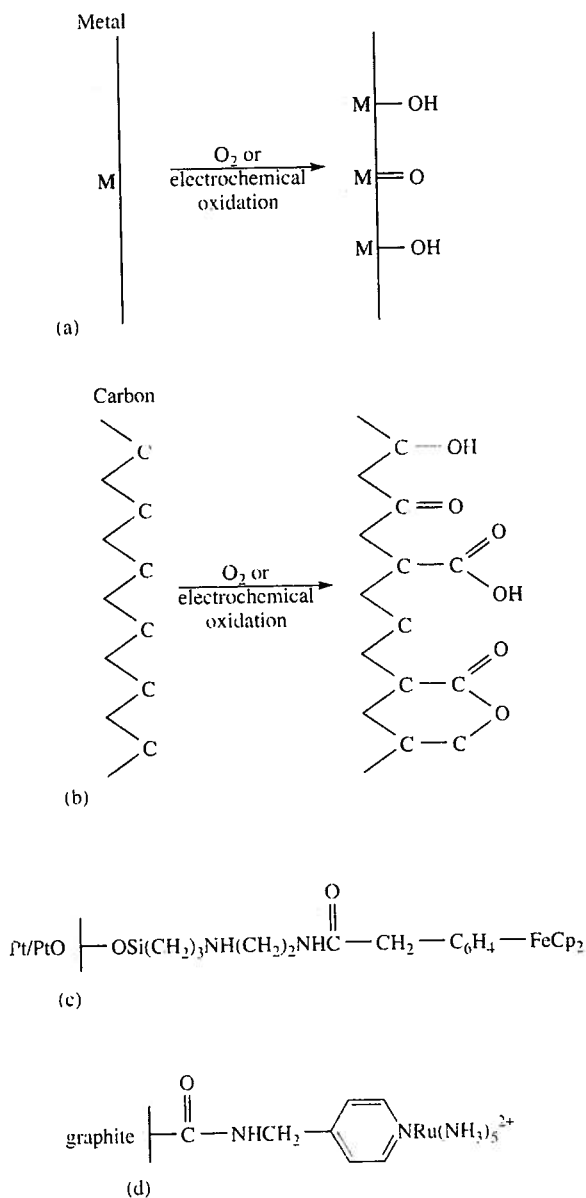
Figure 25-3d shows a commercially available sandwich-type working electrode for voltammetry (or am-

perometry) in flowing streams. The block is made of polyetheretherketone (PEEK) and is available in several formats with different size electrodes (3 mm and 6 mm; see the blue area in the figure) and various arrays (dual 3 mm and quad 2 mm). See Figure 25-17 for a diagram showing how the electrodes are used in flowing streams. The working electrodes may be made of glassy carbon, carbon paste, gold, copper, nickel, platinum, or other suitable custom materials.

25B-2 Modified Electrodes

An active area of research in electrochemistry is the development of electrodes produced by chemical modification of various conductive substrates.⁸ Such electrodes have been tailored to accomplish a broad range of functions. Modifications include applying irreversibly adsorbing substances with desired functionalities, covalent bonding of components to the surface, and coating the electrode with polymer films or films of other substances. The covalent attachment process is shown in Figure 25-5 for a metallic electrode and a carbon electrode. First, the surface of the electrode is oxidized to create functional groups on the surface as shown in Figure 25-5a and b. Then, linking agents such as organosilanes (Figure 25-5c) or amines (Figure 25-5d) are attached to the surface prior to attaching the target group. Polymer films can be prepared from dissolved polymers by dip coating, spin coating, electrodeposition, or covalent attachment. They can also be produced from the monomer by thermal, plasma, pho-

⁸For more information, see R. W. Murray, "Molecular Design of Electrode Surfaces," *Techniques in Chemistry*, Vol. 22, W. Weissberger, founding ed., New York: Wiley, 1992; A. J. Bard, *Integrated Chemical Systems*, New York: Wiley, 1994.



Functional groups formed on (a) a metal or (b) a carbon surface by oxidation. (With permission from A. J. Bard, *Integrated Chemical Systems*, New York: Wiley, 1994.) (c) A linking agent such as the organosilane shown is often bonded to the functionalized surface. Reactive components, such as ferrocenes, viologens, and metal bipyridine complexes, are then attached to form the modified surfaces. A Pt electrode is shown with a ferrocene attached. (With permission from J. R. Lenhard and R. W. Murray, *J. Am. Chem. Soc.*, **1978**, *100*, 7870.) In (d), a graphite electrode is shown with attached py-Ru(NH₃)₅. (With permission from C. A. Koval and F. C. Anson, *Anal. Chem.*, **1978**, *50*, 223.)

tochemical, or electrochemical polymerization methods. Immobilized enzyme biosensors, such as the amperometric sensors described in Section 25C-4, are a type of modified electrode. These can be prepared by covalent attachment, adsorption, or gel entrapment. Another mode of attachment for electrode modification is by *self-assembled monolayers*, or SAMs.⁹ In the most common procedure, a long-chain hydrocarbon with a thiol group at one end and an amine or carboxyl group at the other is applied to a pristine gold or mercury film electrode. The hydrocarbon molecules assemble themselves into a highly ordered array with the thiol group attached to the metal surface and the chosen functional group exposed. The arrays may then be further functionalized by covalent attachment or adsorption of the desired molecular species.

Modified electrodes have many applications. A primary interest has been in the area of electrocatalysis. In this application, electrodes capable of reducing oxygen to water have been sought for use in fuel cells and batteries. Another application is in the production of electrochromic devices that change color on oxidation and reduction. Such devices are used in displays or *smart windows* and *mirrors*. Electrochemical devices that could serve as molecular electronic devices, such as diodes and transistors, are also under intense study. Finally, the most important analytical use for such electrodes is as analytical sensors selective for a particular species or functional group (see Figure 1-7).

Figure 25-6 illustrates the appearance of a typical linear-scan voltammogram for an electrolysis involving the reduction of an analyte species A to give a product P at a mercury film electrode. Here, the working electrode is assumed to be connected to the negative terminal of the linear-scan generator so that the applied potentials are given a negative sign as shown. By convention, cathodic currents are taken to be positive, whereas anodic currents are given a negative sign.¹⁰ In this hypothetical experiment, the solution is assumed to be about 10⁻⁴ M in A, zero M in P, and 0.1 M in

⁹H. O. Finklea, in *Electroanalytical Chemistry: A Series of Advances*, A. J. Bard and I. Rubinstein, eds., Vol. 19, pp. 109–335. New York: Dekker, 1996.

¹⁰This convention, which originated from early polarographic studies, is not universally accepted. Many workers prefer to assign a positive sign to anodic currents. When reading the literature, it is important to establish which convention is being used. See A. J. Bard and L. R. Faulkner, *Electrochemical Methods*, 2nd ed., p. 6. New York: Wiley, 2001.

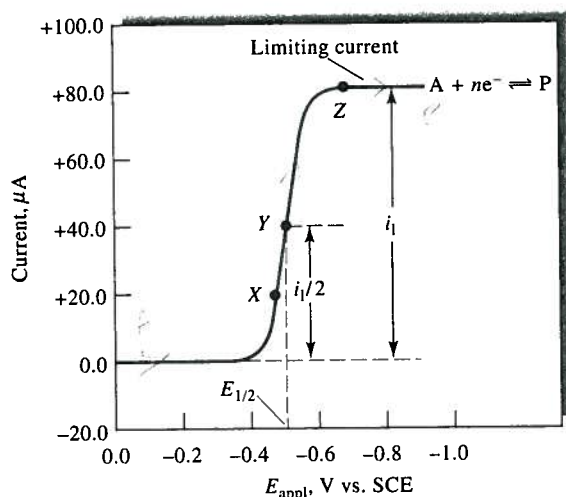
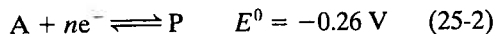


FIGURE 25-6 Linear-sweep voltammogram for the reduction of a hypothetical species A to give a product P. The limiting current i_l is proportional to the analyte concentration and is used for quantitative analysis. The half-wave potential $E_{1/2}$ is related to the standard potential for the half-reaction and is often used for qualitative identification of species. The half-wave potential is the applied potential at which the current i is $i_l/2$.

KCl, which serves as the supporting electrolyte. The half-reaction at the working electrode is the reversible reaction



For convenience, we have neglected the charges on A and P and also have assumed that the standard potential for the half-reaction is -0.26 V .

Linear-scan voltammograms generally have a sigmoid shape and are called *voltammetric waves*. The constant current beyond the steep rise is called the diffusion-limited current, or simply the *limiting current* i_l because the rate at which the reactant can be brought to the surface of the electrode by mass-transport processes limits the current. Limiting currents are usually directly proportional to reactant concentration. Thus, we may write

$$i_l = kc_A$$

where c_A is the analyte concentration and k is a constant. Quantitative linear-scan voltammetry relies on this relationship.

The potential at which the current is equal to one half the limiting current is called the *half-wave potential* and given the symbol $E_{1/2}$. After correction for the

reference electrode potential (0.242 V with a saturated calomel electrode), the half-wave potential is closely related to the standard potential for the half-reaction but is usually not identical to it. Half-wave potentials are sometimes useful for identification of the components of a solution.

Reproducible limiting currents can be achieved rapidly when either the analyte solution or the working electrode is in continuous and reproducible motion. Linear-scan voltammetry in which the solution or the electrode is in constant motion is called *hydrodynamic voltammetry*. In this chapter, we will focus much of our attention on hydrodynamic voltammetry.

25B-4 Circuit Model of a Working Electrode

It is often useful and instructive to represent the electrochemical cell as an electrical circuit that responds to excitation in the same way as the cell. In this discussion, we focus only on the working electrode and assume that the counter electrode is a large inert electrode, that it is nonpolarizable, and that it serves only to make contact with the analyte solution. Figure 25-7 shows a schematic of three of a number of possible circuit models for the electrochemical cell. In Figure 25-7a, we present the *Randles circuit*,¹¹ which consists of the solution resistance R_Ω , the double-layer capacitance C_d , and the *faradaic impedance* Z_f . The physical diagram of the electrode above the circuit shows the correspondence between the circuit elements and the characteristics of the electrode. Although R_Ω and C_d represent the behavior of real electrodes quite accurately over a broad frequency range, and their values are independent of frequency, the faradaic impedance does not. This is because, in general, Z_f must model any electron- and mass-transfer processes that occur in the cell, and these processes are frequency dependent. The simplest representation of the faradaic impedance contains a series resistance R_s and the *pseudocapacitance* C_s (Figure 25-7b), which is so called because of its frequency dependence.¹²

In the past, clever methods were devised to determine values for R_Ω and C_d . For example, suppose that we apply a small-amplitude sinusoidal excitation signal to a cell containing the working electrode represented by Figure 25-7b. We further assume that the value of the applied voltage is insufficient to initiate faradaic

¹¹ J. E. B. Randles, *Disc. Faraday Soc.*, 1947, 1, 11.

¹² A. J. Bard and L. R. Faulkner, *Electrochemical Methods*, 2nd ed., p. 376, New York: Wiley, 2001.

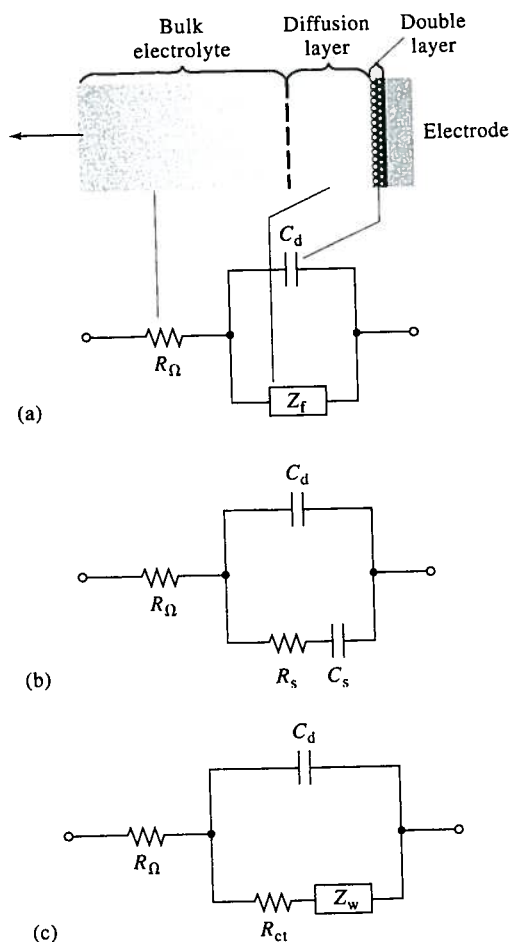


FIGURE 25-7 Circuit model of an electrochemical cell. R_Ω is the cell resistance, C_d is the double-layer capacitance, and Z_f is the faradaic impedance, which may be represented by either of the equivalent circuits shown. R_s is the cell resistance, C_s is the so-called pseudocapacitance, and Z_w is the Warburg impedance. (Adapted from A. J. Bard and L. R. Faulkner, *Electrochemical Methods*, 2nd ed., p. 376, New York: Wiley, 2001. Reprinted by permission of John Wiley & Sons, Inc.)

processes. At relatively high frequencies, the capacitive reactance $X_C = 1/(2\pi fC_d)$ will be quite small (see Section 2B-4), and C_d acts essentially as a short circuit. If we then measure the peak current I_p in the circuit, we find $R_\Omega = V_p/I_p$. This is actually a widely used method for determining solution conductance $G = 1/R_\Omega = I_p/V_p$. In a similar way, each of the circuit elements of the model can be isolated and their values determined by artful application of *ac* circuit measurement techniques.

Figure 25-7c shows a third model for the working electrode in which the faradaic impedance is represented as the series combination of the charge-transfer resistance R_{ct} and the Warburg impedance Z_w . The charge-transfer resistance is given by $R_{ct} = -\eta/i$, where η is the overpotential for the faradaic process occurring at the working electrode (see Section 22E-2), and i is the current.¹³ The Warburg impedance is a frequency-dependent circuit analog of the resistance of the working electrode to mass transport of analyte molecules across the electrode-solution interface. When experimental conditions are such that the Warburg impedance can be neglected, the charge-transfer resistance can be easily measured, for example, at excitation frequencies near zero.

With modern computerized frequency-analysis instrumentation and software, it is possible to acquire impedance data on cells and extract the values for all components of the circuit models of Figure 25-7. This type of analysis, which is called *electrochemical impedance spectroscopy*, reveals the nature of the faradaic processes and often aids in the investigation of the mechanisms of electron-transfer reactions.¹⁴ In the section that follows, we explore the processes at the electrode-solution interface that give rise to the faradaic impedance.

25C HYDRODYNAMIC VOLTAMMETRY

Hydrodynamic voltammetry is performed in several ways. In one method the solution is stirred vigorously while it is in contact with a fixed working electrode. A typical cell for hydrodynamic voltammetry is pictured in Figure 25-8. In this cell, stirring is accomplished with an ordinary magnetic stirrer. Another approach is to rotate the working electrode at a constant high speed in the solution to provide the stirring action (Figure 25-21a). Still another way of doing hydrodynamic voltammetry is to pass an analyte solution through a tube fitted with a working electrode (Figure 25-17). The last technique is widely used for detecting oxidizable or reducible analytes as they exit from a liquid chromatographic column (Section 28C-6) or a flow-injection manifold.

As described in Section 22E-3, during an electrolysis, reactant is carried to the surface of an electrode by

¹³ *Ibid.*, p. 102.

¹⁴ *Ibid.*, pp. 383–88; M. E. Orazem and B. Tribollet, *Electrochemical Impedance Spectroscopy*, New York: Wiley, 2006.

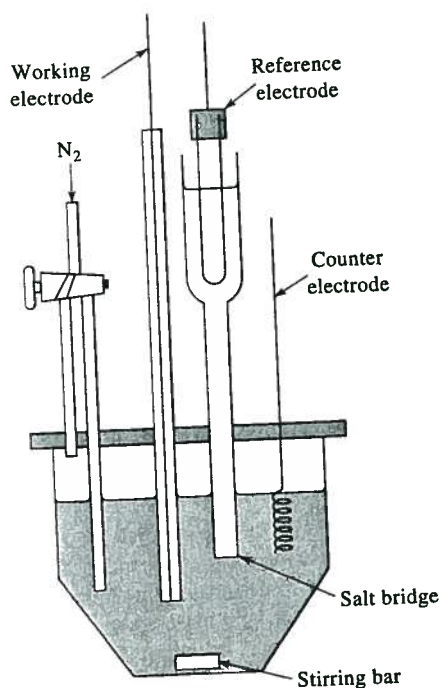


FIGURE 25-8 A three-electrode cell for hydrodynamic voltammetry.

three mechanisms: *migration* under the influence of an electric field, *convection* resulting from stirring or vibration, and *diffusion* due to concentration differences between the film of liquid at the electrode surface and the bulk of the solution. In voltammetry, we attempt to minimize the effect of migration by introducing an excess of an inactive supporting electrolyte. When the concentration of supporting electrolyte exceeds that of the analyte by 50- to 100-fold, the fraction of the total current carried by the analyte approaches zero. As a result, the rate of migration of the analyte toward the electrode of opposite charge becomes essentially independent of applied potential.

25C-1 Concentration Profiles at Electrode Surfaces

Throughout this discussion we will consider that the electrode reaction shown in Equation 25-2 takes place at an electrode in a solution of A that also contains an excess of a supporting electrolyte. We will assume that the initial concentration of A is c_A and that of the product P is zero. We also assume that the reduction



Simulation: Learn more about **diffusion at electrodes.**

reaction is rapid and reversible so that the concentrations of A and P in the film of solution immediately adjacent to the electrode is given at any instant by the Nernst equation:

$$E_{\text{appl}} = E_A^0 - \frac{0.0592}{n} \log \frac{c_P^0}{c_A^0} - E_{\text{ref}} \quad (25-3)$$

where E_{appl} is the potential between the working electrode and the reference electrode and c_P^0 and c_A^0 are the molar concentrations of P and A in a thin layer of solution at the electrode surface only. We also assume that because the electrode is quite small, the electrolysis, over short periods, does not alter the bulk concentration of the solution appreciably. As a result, the concentration of A in the bulk of the solution c_A is unchanged by the electrolysis and the concentration of P in the bulk of the solution c_P continues to be, for all practical purposes, zero ($c_P \approx 0$).

Profiles for Planar Electrodes in Unstirred Solutions

Before describing the behavior of an electrode in this solution under hydrodynamic conditions, it is instructive to consider what occurs when a potential is applied to a planar electrode, such as that shown in Figure 25-3a, in the absence of convection — that is, in an unstirred solution. Under these conditions mass transport of the analyte to the electrode surface occurs by diffusion alone.

Let us assume that a square-wave excitation potential E_{appl} is applied to the working electrode for a period of time t as shown in Figure 25-9a. Let us further assume that E_{appl} is large enough that the ratio c_P^0/c_A^0 in Equation 25-3 is 1000 or greater. Under this condition, the concentration of A at the electrode surface is, for

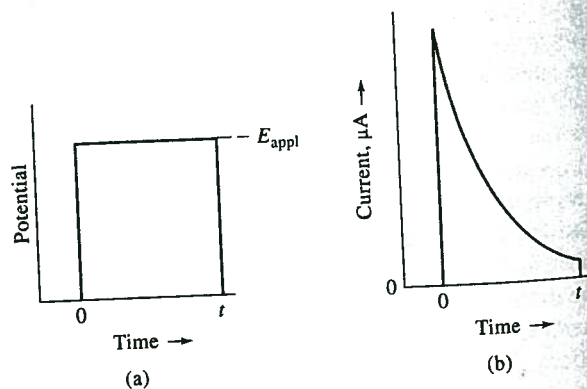


FIGURE 25-9 Current response to a stepped potential for a planar electrode in an unstirred solution. (a) Excitation potential. (b) Current response.

all pra
($c_A^0 \rightarrow 0$)
signal
rises to
tially a
fusion
A into
curs.
of A :
rapid
great
when
the c
Fi
P aft
unde
A (s
ted
face
neo
the
face
cen
mil
ure
the

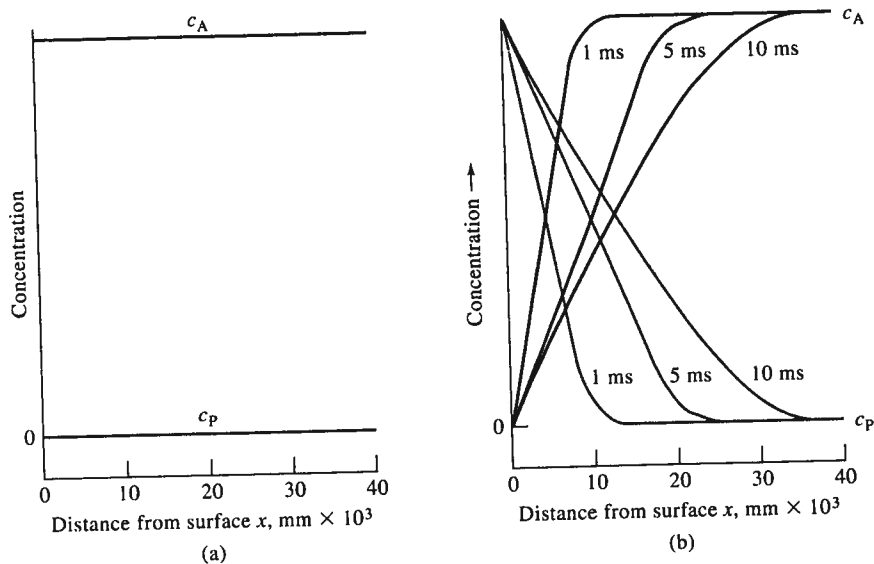


FIGURE 25-10 Concentration distance profiles during the diffusion-controlled reduction of A to give P at a planar electrode. (a) $E_{\text{appl}} = 0$ V. (b) $E_{\text{appl}} =$ point Z in Figure 25-6; elapsed time: 1, 5, and 10 ms.

all practical purposes, immediately reduced to zero ($c_A^0 \rightarrow 0$). The current response to this step-excitation signal is shown in Figure 25-9b. Initially, the current rises to a peak value that is required to convert essentially all of A in the surface layer of solution to P. Diffusion from the bulk of the solution then brings more A into this surface layer where further reduction occurs. The current required to keep the concentration of A at the level required by Equation 25-3 decreases rapidly with time, however, because A must travel greater and greater distances to reach the surface layer where it can be reduced. Thus, as seen in Figure 25-9b, the current drops off rapidly after its initial surge.

Figure 25-10 shows concentration profiles for A and P after 0, 1, 5, and 10 ms of electrolysis in the system under discussion. In this example, the concentration of A (solid black lines) and P (solid blue lines) are plotted as a function of distance from the electrode surface. Figure 25-10a shows that the solution is homogeneous before application of the stepped potential with the concentration of A being c_A at the electrode surface and in the bulk of the solution as well; the concentration of P is zero in both of these regions. One millisecond after application of the potential (Figure 25-10b), the profiles have changed dramatically. At the surface of the electrode, the concentration of A

has been reduced to essentially zero and the concentration of P has increased and become equal to the original concentration of A; that is, $c_P^0 = c_A$. Moving away from the surface, the concentration of A increases linearly with distance and approaches c_A at about 0.01 mm from the surface. A linear decrease in the concentration of P occurs in this same region. As shown in the figure, with time, these concentration gradients extend farther and farther into the solution. The current i required to produce these gradients is proportional to the slopes of the straight-line portions of the solid lines in Figure 25-10b. That is,

$$i = nFAD_A \left(\frac{\partial c_A}{\partial x} \right) \quad (25-4)$$

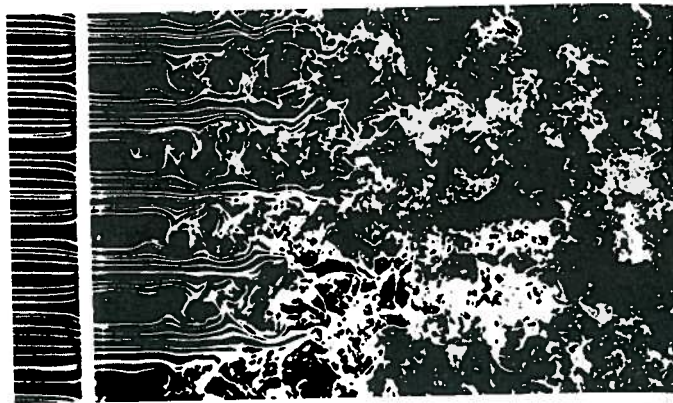
where i is the current in amperes, n is the number of moles of electrons per mole of analyte, F is the faraday, A is the electrode surface area (cm^2), D_A is the diffusion coefficient for A (cm^2/s), and c_A is the concentration of A (mol/cm^3). As shown in Figure 25-10b, these slopes ($\partial c_A / \partial x$) become smaller with time, as does the current. The product $D_A(\partial c_A / \partial x)$ is called the *flux*, which is the number of moles of A per unit time per unit area diffusing to the electrode.

It is not practical to obtain limiting currents with planar electrodes in unstirred solutions because the currents continually decrease with time as the slopes of the concentration profiles become smaller.



Simulation: Learn more about **concentration profiles at electrodes.**

FIGURE 25-11 Visualization of flow patterns in a flowing stream. Turbulent flow, shown on the right, becomes laminar flow as the average velocity decreases to the left. In turbulent flow, the molecules move in an irregular, zigzag fashion and there are swirls and eddies in the movement. In laminar flow, the streamlines become steady as layers of liquid slide by each other in a regular manner. (From *An Album of Fluid Motion*, assembled by Milton Van Dyke, no. 152, photograph by Thomas Corke and Hassan Nagib, Stanford, CA: Parabolic Press, 1982.)

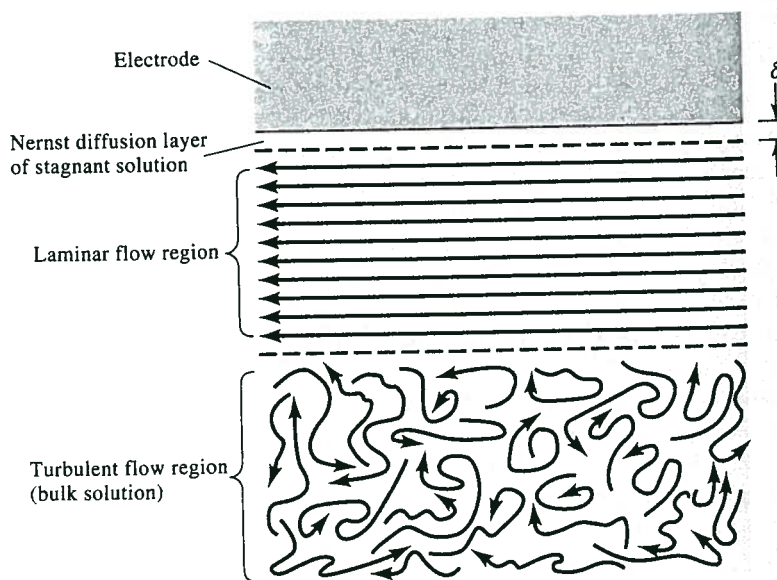


Profiles for Electrodes in Stirred Solutions

Let us now consider concentration-distance profiles when the reduction described in the previous section is performed at an electrode immersed in a solution that is stirred vigorously. To understand the effect of stirring, we must develop a picture of liquid flow patterns in a stirred solution containing a small planar electrode. We can identify two types of flow depending on the average flow velocity, as shown in Figure 25-11. *Laminar flow* occurs at low flow velocities and has smooth and regular motion as depicted on the left in the figure. *Turbulent flow*, on the other hand, happens at high velocities and has irregular, fluctuating motion as shown on the right. In a stirred electrochemical cell, we have a region of turbulent flow in the bulk of solution far from the electrode and a region of laminar flow

close to the electrode. These regions are illustrated in Figure 25-12. In the laminar-flow region, the layers of liquid slide by one another in a direction parallel to the electrode surface. Very near the electrode, at a distance δ centimeters from the surface, frictional forces give rise to a region where the flow velocity is essentially zero. The thin layer of solution in this region is a stagnant layer called the *Nernst diffusion layer*. It is only within the stagnant Nernst diffusion layer that the concentrations of reactant and product vary as a function of distance from the electrode surface and that there are concentration gradients. That is, throughout the laminar-flow and turbulent-flow regions, convection maintains the concentration of A at its original value and the concentration of P at a very low level.

FIGURE 25-12 Flow patterns and regions of interest near the working electrode in hydrodynamic voltammetry.



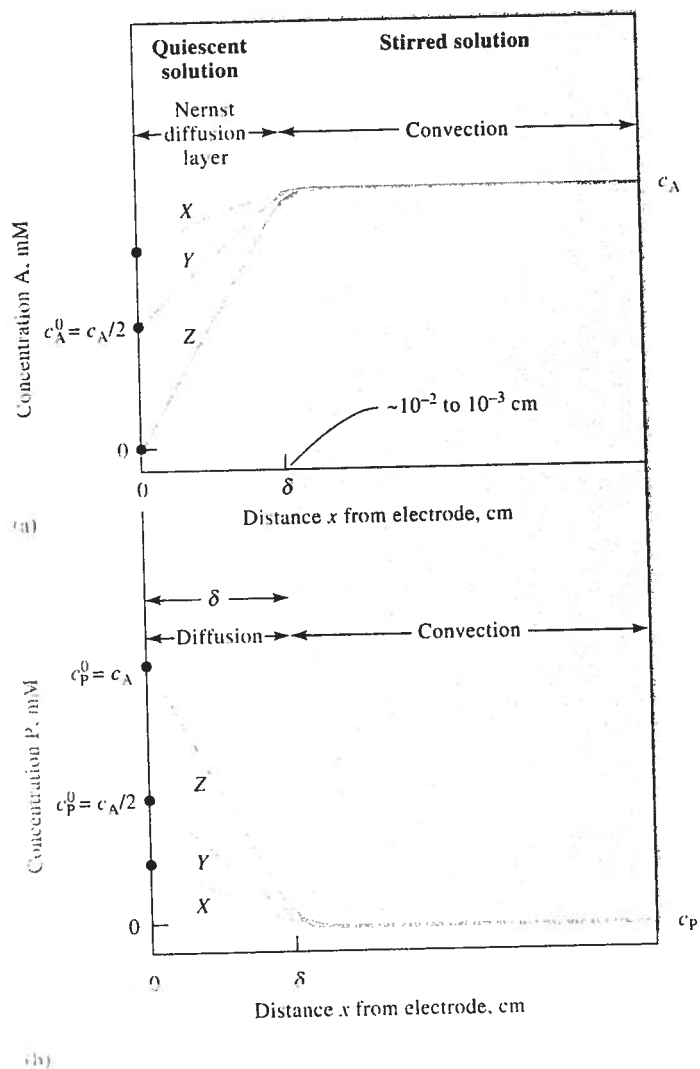


Figure 25-13 Concentration profiles at an electrode-solution interface during the electrolysis $A + ne^- \rightarrow P$ from a stirred solution of A. See Figure 25-6 for potentials corresponding to curves X, Y, and Z.

Figure 25-13 shows two sets of concentration profiles for A and P at three potentials shown as X, Y, and Z in Figure 25-6. In Figure 25-13a, the solution is divided into two regions. One makes up the bulk of the solution and consists of both the turbulent- and laminar-flow regions shown in Figure 25-12, where mass transport takes place by mechanical convection brought about by the stirrer. The concentration of A throughout this region is c_A , whereas c_P is essentially zero. The second region is the Nernst diffusion layer, which is immediately adjacent to the electrode surface and has a thickness of δ centimeters. Typically, δ ranges from 10^{-2} to 10^{-3} cm, depending on the efficiency of the stirring and the viscosity of the liquid. Within the static diffusion layer, mass transport takes

place by diffusion alone, just as was the case with the unstirred solution. With the stirred solution, however, diffusion is limited to a narrow layer of liquid, which even with time cannot extend indefinitely into the solution. As a result, steady, diffusion-controlled currents appear shortly after applying a voltage.

As is shown in Figure 25-13, at potential X, the equilibrium concentration of A at the electrode surface has been reduced to about 80% of its original value and the equilibrium concentration P has increased by an equivalent amount: that is, $c_P^0 = c_A - c_A^0$. At potential Y, which is the half-wave potential, the equilibrium concentrations of the two species at the surface are approximately the same and equal to $c_A/2$. Finally, at potential Z and beyond, the surface concentration of A

approaches zero, and that of P approaches the original concentration of A, c_A . Thus, at potentials more negative than Z, essentially all A ions entering the surface layer are instantaneously reduced to P. As is shown in Figure 25-13b, at potentials greater than Z the concentration of P in the surface layer remains constant at $c_P^0 = c_A$ because of diffusion of P back into the stirred region.

25C-2 Voltammetric Currents

The current at any point in the electrolysis we have just discussed is determined by the rate of transport of A from the outer edge of the diffusion layer to the electrode surface. Because the product of the electrolysis P diffuses from the surface and is ultimately swept away by convection, a continuous current is required to maintain the surface concentrations demanded by the Nernst equation. Convection, however, maintains a constant supply of A at the outer edge of the diffusion layer. Thus, a steady-state current results that is determined by the applied potential. This current is a quantitative measure of how fast A is being brought to the surface of the electrode, and this rate is given by $\partial c_A / \partial x$ where x is the distance in centimeters from the electrode surface. For a planar electrode, the current is given by Equation 25-4.

Note that $\partial c_A / \partial x$ is the slope of the initial part of the concentration profiles shown in Figure 25-13a, and these slopes can be approximated by $(c_A - c_A^0) / \delta$. When this approximation is valid, Equation 25-4 reduces to

$$i = \frac{nFAD_A}{\delta} (c_A - c_A^0) = k_A (c_A - c_A^0) \quad (25-5)$$

where the constant k_A is equal to $nFAD_A / \delta$.

Equation 25-5 shows that as c_A^0 becomes smaller as a result of a larger negative applied potential the current increases until the surface concentration approaches zero, at which point the current becomes constant and independent of the applied potential. Thus, when $c_A^0 \rightarrow 0$, the current becomes the limiting current i_l , and Equation 25-5 reduces to Equation 25-6.¹⁵

$$i_l = \frac{nFAD_A}{\delta} c_A = k_A c_A \quad (25-6)$$

¹⁵Careful analysis of the units of the variables in this equation leads to

$$n \left(\frac{\text{mol e}^-}{\text{mol analyte}} \right) F \left(\frac{\text{C}}{\text{mol e}^-} \right) A (\text{cm}^2) D_A \left(\frac{\text{cm}^2}{\text{s}} \right) c_A \left(\frac{\text{mol analyte}}{\text{cm}^3} \right) / \delta (\text{cm})$$

$$= i_l \left(\frac{\text{C}}{\text{s}} \right)$$

By definition, one coulomb per second is one ampere.

This derivation is based on an oversimplified picture of the diffusion layer in that the interface between the moving and stationary layers is viewed as a sharply defined edge where transport by convection ceases and transport by diffusion begins. Nevertheless, this simplified model does provide a reasonable approximation of the relationship between current and the variables that affect the current.

Current-Voltage Relationships for Reversible Reactions

To develop an equation for the sigmoid curve shown in Figure 25-6, we substitute Equation 25-6 into Equation 25-5 and rearrange, which gives

$$c_A^0 = \frac{i_l - i}{k_A} \quad (25-7)$$

The surface concentration of P can also be expressed in terms of the current by using a relationship similar to Equation 25-5. That is,

$$i = -\frac{nFAD_P}{\delta} (c_P - c_P^0) \quad (25-8)$$

where the minus sign results from the negative slope of the concentration profile for P. Note that D_P is now the diffusion coefficient of P. But we have said earlier that throughout the electrolysis the concentration of P approaches zero in the bulk of the solution and, therefore, when $c_P \approx 0$,

$$i = \frac{-nFAD_P c_P^0}{\delta} = k_P c_P^0 \quad (25-9)$$

where $k_P = -nFAD_P / \delta$. Rearranging gives

$$c_P^0 = i / k_P \quad (25-10)$$

Substituting Equations 25-7 and 25-10 into Equation 25-3 yields, after rearrangement,

$$E_{\text{appl}} = E_A^0 - \frac{0.0592}{n} \log \frac{k_A}{k_P} - \frac{0.0592}{n} \log \frac{i}{i_l - i} - E_{\text{ref}} \quad (25-11)$$

When $i = i_l / 2$, the third term on the right side of this equation becomes equal to zero, and, by definition, E_{appl} is the half-wave potential. That is,

$$E_{\text{appl}} = E_{1/2} = E_A^0 - \frac{0.0592}{n} \log \frac{k_A}{k_P} - E_{\text{ref}} \quad (25-12)$$

Substituting this expression into Equation 25-11 gives an expression for the voltammogram in Figure 25-6. That is,

Offer
tion 2
speci

Curr
for Ir

Man
those
whic
To d
ditio
of tl
tials
pen:
line:
proc
anal

Volt

The
pen
a ve
way
sho
mix
diff
cur
the
proc
ual
0.2
de
0.2
pr

Ar

Vc

A

te

ill

tr

in

ol

el

$$E_{\text{appl}} = E_{1/2} - \frac{0.0592}{n} \log \frac{i}{i_1 - i} \quad (25-13)$$

Often, the ratio k_A/k_P in Equation 25-11 and in Equation 25-12 is nearly unity, so that we may write for the species A

$$E_{1/2} \approx E_A^0 - E_{\text{ref}} \quad (25-14)$$

Current-Voltage Relationships for Irreversible Reactions

Many voltammetric electrode processes, particularly those associated with organic systems, are irreversible, which leads to drawn-out and less well-defined waves. To describe these waves quantitatively requires an additional term in Equation 25-12 involving the activation energy of the reaction to account for the kinetics of the electrode process. Although half-wave potentials for irreversible reactions ordinarily show some dependence on concentration, diffusion currents remain linearly related to concentration. Some irreversible processes can, therefore, be adapted to quantitative analysis if suitable calibration standards are available.

Voltammograms for Mixtures of Reactants

The reactants of a mixture generally behave independently of one another at a working electrode. Thus, a voltammogram for a mixture is just the sum of the waves for the individual components. Figure 25-14 shows the voltammograms for a pair of two-component mixtures. The half-wave potentials of the two reactants differ by about 0.1 V in curve A and by about 0.2 V in curve B. Note that a single voltammogram may permit the quantitative determination of two or more species provided there is sufficient difference between succeeding half-wave potentials to permit evaluation of individual diffusion currents. Generally, a difference of 0.1 to 0.2 V is required if the more easily reducible species undergoes a two-electron reduction; a minimum of about 0.3 V is needed if the first reduction is a one-electron process.

Anodic and Mixed Anodic-Cathodic Voltammograms

Anodic waves as well as cathodic waves are encountered in voltammetry. An example of an anodic wave is illustrated in curve A of Figure 25-15, where the electrode reaction is the oxidation of iron(II) to iron(III) in the presence of citrate ion. A limiting current is observed at about +0.1 V (versus a saturated calomel electrode [SCE]), which is due to the half-reaction

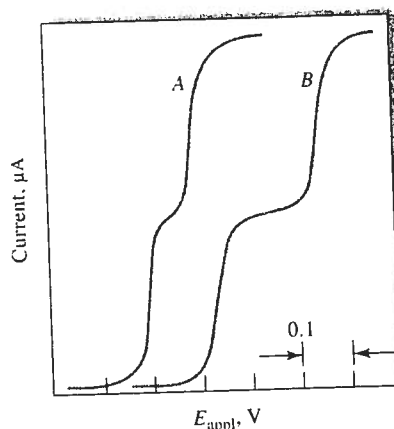
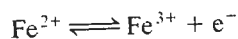


FIGURE 25-14 Voltammograms for two-component mixtures. Half-wave potentials differ by 0.1 V in curve A, and by 0.2 V in curve B.



As the potential is made more negative, a decrease in the anodic current occurs; at about -0.02 V, the current becomes zero because the oxidation of iron(II) ion has ceased.

Curve C represents the voltammogram for a solution of iron(III) in the same medium. Here, a cathodic wave results from reduction of iron(III) to iron(II). The half-wave potential is identical with that for the anodic wave, indicating that the oxidation and reduc-

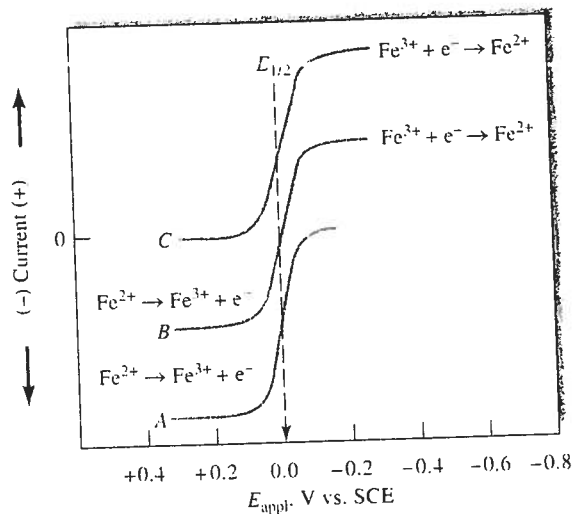


FIGURE 25-15 Voltammetric behavior of iron(II) and iron(III) in a citrate medium. Curve A: anodic wave for a solution in which $c_{\text{Fe}^{2+}} = 1 \times 10^{-4}$ M. Curve B: anodic-cathodic wave for a solution in which $c_{\text{Fe}^{2+}} = c_{\text{Fe}^{3+}} = 0.5 \times 10^{-4}$ M. Curve C: cathodic wave for a solution in which $c_{\text{Fe}^{3+}} = 1 \times 10^{-4}$ M.

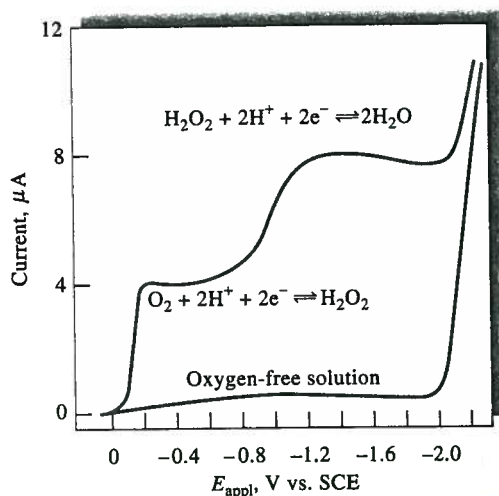


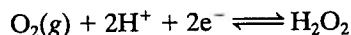
FIGURE 25-16 Voltammogram for the reduction of oxygen in an air-saturated 0.1-M KCl solution. The lower curve is for a 0.1-M KCl solution in which the oxygen is removed by bubbling nitrogen through the solution.

tion of the two iron species are perfectly reversible at the working electrode.

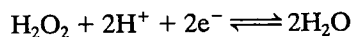
Curve *B* is the voltammogram of an equimolar mixture of iron(II) and iron(III). The portion of the curve below the zero-current line corresponds to the oxidation of the iron(II); this reaction ceases at an applied potential equal to the half-wave potential. The upper portion of the curve is due to the reduction of iron(III).

25C-3 Oxygen Waves

Dissolved oxygen is easily reduced at many working electrodes. Thus, as shown in Figure 25-16, an aqueous solution saturated with air exhibits two distinct oxygen waves. The first results from the reduction of oxygen to hydrogen peroxide:



The second wave corresponds to the further reduction of the hydrogen peroxide:



Because both reactions are two-electron reductions, the two waves are of equal height.

Voltammetric measurements offer a convenient and widely used method for determining dissolved oxygen in solutions. However, the presence of oxygen often interferes with the accurate determination of other species. Thus, oxygen removal is usually the first step in amperometric procedures. Oxygen can be re-

moved by passing an inert gas through the analyte solution for several minutes (*sparging*). A stream of the same gas, usually nitrogen, is passed over the surface of the solution during analysis to prevent reabsorption of oxygen. The lower curve in Figure 25-16 is a voltammogram of an oxygen-free solution.

25C-4 Applications of Hydrodynamic Voltammetry

The most important uses of hydrodynamic voltammetry include (1) detection and determination of chemical species as they exit from chromatographic columns or flow-injection apparatus; (2) routine determination of oxygen and certain species of biochemical interest, such as glucose, lactose, and sucrose; (3) detection of end points in coulometric and volumetric titrations; and (4) fundamental studies of electrochemical processes.

Voltammetric Detectors in Chromatography and Flow-Injection Analysis

Hydrodynamic voltammetry is widely used for detection and determination of oxidizable or reducible compounds or ions that have been separated by liquid

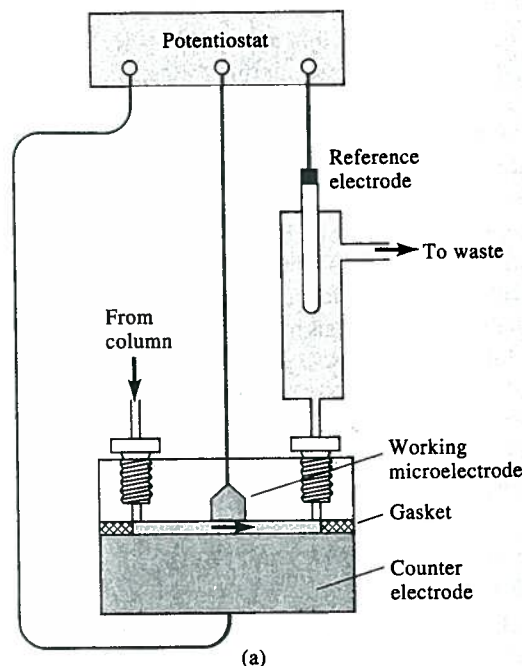
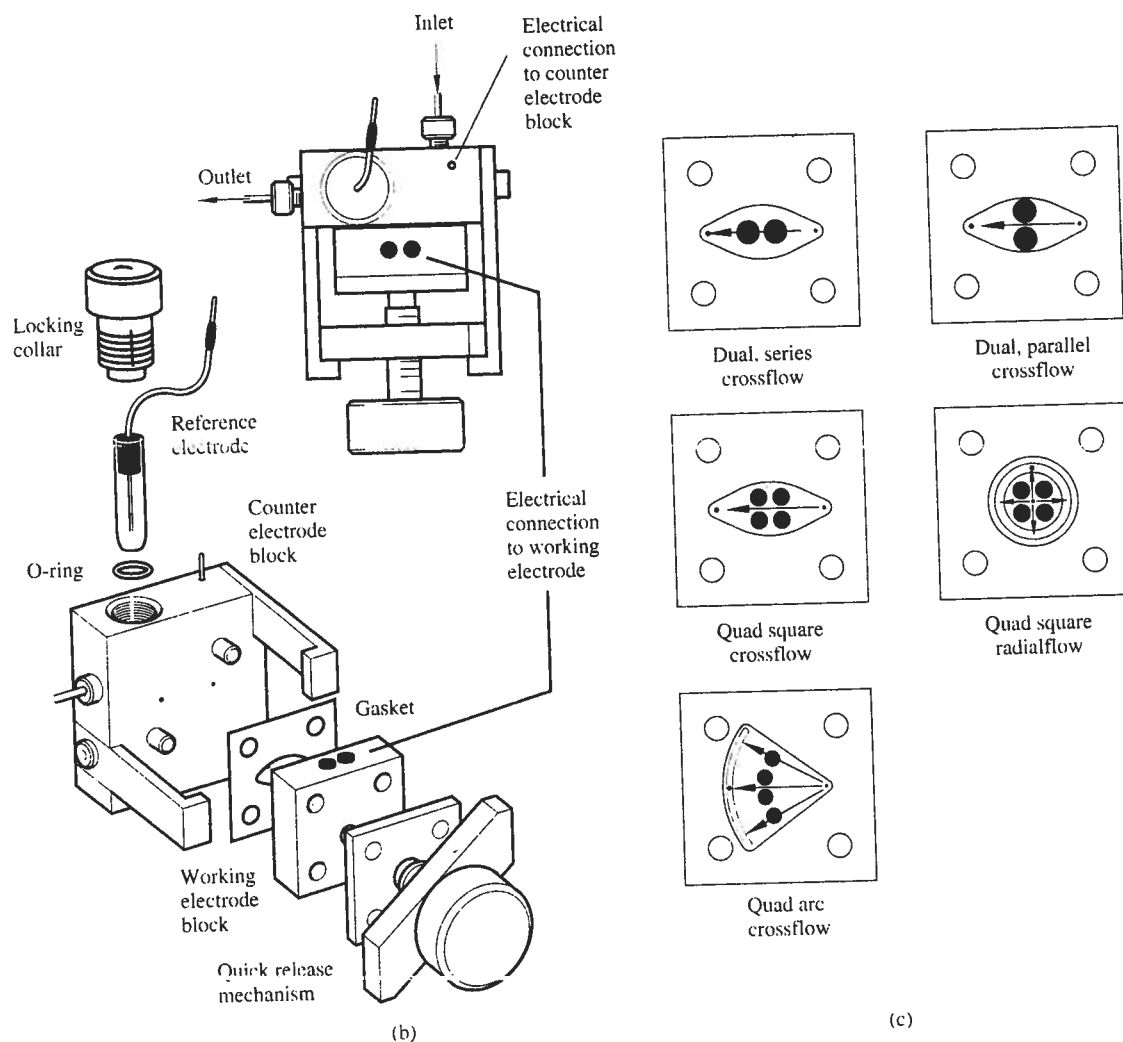


FIGURE 25-17 (a) A schematic of a voltammetric system for detecting electroactive species as they elute from a column. The cell volume is determined by the thickness of the gasket.



(continued) (b) Detail of a commercial flow cell assembly. (c) Configurations of working electrode blocks. Arrows show the direction of flow in the cell. ([b] and [c] courtesy of Bioanalytical Systems, Inc., West Lafayette, IN.)

chromatography or that are produced by flow-injection methods.¹⁶ A thin-layer cell such as the one shown schematically in Figure 25-17a is used in these applications. The working electrode in these cells is usually embedded in the wall of an insulating block separated

¹⁶Voltammetric detectors are a particular type of transducer called *limiting-current transducers*. In this discussion and subsequent discussions involving voltammetric transducers, we use the more common term *voltammetric detector*. When a voltammetric transducer is inherently selective for a particular species by virtue of control of various experimental variables or when it is covered with a chemically selective layer of polymer or other membranous material, we refer to it as a *voltammetric sensor*. For a discussion of transducers, detectors, sensors, and their definitions, see Section 1C-4.

from a counter electrode by a thin spacer as shown. The volume of such a cell is typically 0.1 to 1 μL . A voltage corresponding to the limiting-current region for analytes is applied between the working electrode and a silver-silver chloride reference electrode that is located downstream from the detector. We present an exploded view of a commercial flow cell in Figure 25-17b, which shows clearly how the sandwiched cell is assembled and held in place by the quick-release mechanism. A locking collar in the counter electrode block, which is electrically connected to the potentiostat, retains the reference electrode. Five different configurations of working electrode are shown in

Figure 25-17c. These configurations permit optimization of detector sensitivity under a variety of experimental conditions. Working electrode blocks and electrode materials are described in Section 25B-1. This type of application of voltammetry (or amperometry) has detection limits as low as 10^{-9} to 10^{-10} M. We discuss voltammetric detection for liquid chromatography in more detail in Section 28C-6.

Voltammetric and Amperometric Sensors

In Section 23F-2, we described how the specificity of potentiometric sensors could be enhanced by applying molecular recognition layers to the electrode surfaces. There has been much research in recent years in applying the same concepts to voltammetric electrodes.¹⁷ A number of voltammetric systems are available commercially for the determination of specific species in industrial, biomedical, environmental, and research applications. These devices are sometimes called electrodes or detectors but are, in fact, complete voltammetric cells and are better referred to as sensors. In the sections that follow, we describe two commercially available sensors and one that is under development in this rapidly expanding field.

Oxygen Sensors. The determination of dissolved oxygen in a variety of aqueous environments, such as seawater, blood, sewage, effluents from chemical plants, and soils, is of tremendous importance to industry, biomedical and environmental research, and clinical medicine. One of the most common and convenient methods for making such measurements is with the Clark oxygen sensor, which was patented by L. C. Clark Jr. in 1956.¹⁸ A schematic of the Clark oxygen sensor is shown in Figure 25-18. The cell consists of a cathodic platinum-disk working electrode embedded in a centrally located cylindrical insulator. Surrounding the lower end of this insulator is a ring-shaped silver anode. The tubular insulator and electrodes are mounted inside a second cylinder that contains a buffered solution of potassium chloride. A thin ($\sim 20 \mu\text{m}$), replaceable, oxygen-permeable membrane of Teflon or polyethylene is held in place at the bottom end of the tube by an O-ring. The thickness of the electrolyte solution between the cathode and the membrane is approximately $10 \mu\text{m}$.

¹⁷For a recent review of electrochemical sensors, see E. Bakker and Yu Qin, *Anal. Chem.*, **2006**, *78*, 3965.

¹⁸For a detailed discussion of the Clark oxygen sensor, see M. L. Hitchman, *Measurement of Dissolved Oxygen*, Chaps. 3–5, New York: Wiley, 1978.

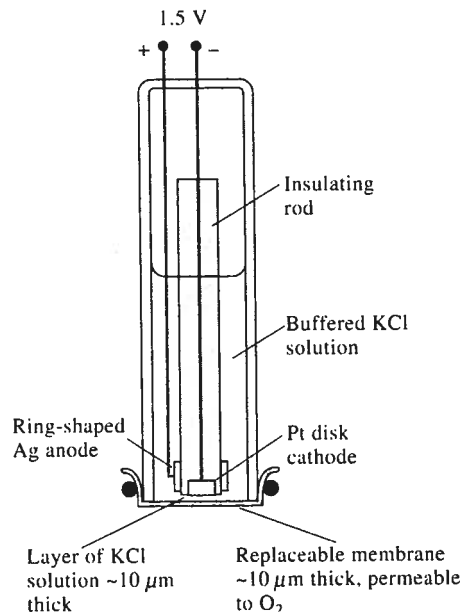
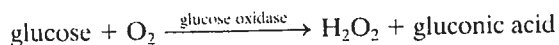


FIGURE 25-18 The Clark voltammetric oxygen sensor. Cathodic reaction: $\text{O}_2 + 4\text{H}^+ + 4\text{e}^- \rightleftharpoons 2\text{H}_2\text{O}$. Anodic reaction: $\text{Ag} + \text{Cl}^- \rightleftharpoons \text{AgCl}(\text{s}) + \text{e}^-$.

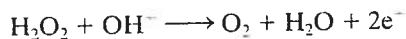
When the oxygen sensor is immersed in a flowing or stirred solution of the analyte, oxygen diffuses through the membrane into the thin layer of electrolyte immediately adjacent to the disk cathode, where it diffuses to the electrode and is immediately reduced to water. In contrast with a normal hydrodynamic electrode, two diffusion processes are involved—one through the membrane and the other through the solution between the membrane and the electrode surface. For a steady-state condition to be reached in a reasonable period (10 to 20 s), the thickness of the membrane and the electrolyte film must be $20 \mu\text{m}$ or less. Under these conditions, it is the rate of equilibration of the transfer of oxygen across the membrane that determines the steady-state current that is reached.

Enzyme-Based Sensors. A number of enzyme-based voltammetric sensors are available commercially. An example is a glucose sensor that is widely used in clinical laboratories for the routine determination of glucose in blood serum. This device is similar in construction to the oxygen sensor shown in Figure 25-18. The membrane in this case is more complex and consists of three layers. The outer layer is a polycarbonate film that is permeable to glucose but impermeable to proteins and other constituents of blood. The middle layer

is an immobilized enzyme (see Section 23F-2), glucose oxidase in this example. The inner layer is a cellulose acetate membrane, which is permeable to small molecules, such as hydrogen peroxide. When this device is immersed in a glucose-containing solution, glucose diffuses through the outer membrane into the immobilized enzyme, where the following catalytic reaction occurs:



The hydrogen peroxide then diffuses through the inner layer of membrane and to the electrode surface, where it is oxidized to give oxygen. That is,



The resulting current is directly proportional to the glucose concentration of the analyte solution. A variation on this type of sensor is often found in home glucose monitors widely used by diabetic patients. This device is one of the largest-selling chemical instruments in the world.¹⁹

Several other sensors are available that are based on the voltammetric measurement of hydrogen peroxide produced by enzymatic oxidations of other species of clinical interest. These analytes include sucrose, lactose, ethanol, and L-lactate. A different enzyme is, of course, required for each species. In some cases, enzyme electrodes can be based on measuring oxygen or on measuring pH as discussed in Section 23F-2.

Immunosensors. Sensor specificity is often achieved by using molecular recognition elements that react exclusively with the analyte. Antibodies are proteins that have exceptional specificity toward analytes and are the recognition elements most commonly used in *immunosensors*.²⁰ Immunosensors are typically fabricated by immobilizing antibodies on the sensor surface either through adsorption, covalent attachment, polymer entrapment, or other methods.

A variety of assay formats are used with immunosensors. One of the most common methods uses two antibodies, one that is immobilized on the sensor surface and is used to capture the target analyte, and one that is labeled and is used to detect the captured analyte (a *sandwich assay*). Traditionally, radionuclides were

used as labels in immunoassays, but these have largely been replaced by more convenient labels such as fluorescent molecules and enzymes. Thus, immunosensors can use a variety of detection methods, such as optical and electrochemical techniques. More recently, label-free immunosensors have been developed based on piezoelectric (Section 1C-4), surface plasmon resonance (Section 21E-1), and other detection strategies.

Figure 25-19 shows a scheme and an amperometric biosensor for determining specific proteins using a sandwich assay.²¹ In this scheme (Figure 25-19a), an antibody appropriate for the desired analyte is immobilized on the surface of an electrode (A). In this example, the antibody is immobilized by physical adsorption.²² When the electrode is in contact with a solution containing the analyte, which is represented as blue triangles in the figure, it binds preferentially with the antibody (B). The electrode is then rinsed and brought into contact with a second antibody that has been tagged, or labeled, which is indicated by the stars in the figure (C). In this example, the antibody is tagged with the enzyme alkaline phosphatase, which catalyzes the conversion of hydroquinone diphosphate to hydroquinone. When a voltage of 320 mV versus Ag-AgCl is applied to the working electrode, hydroquinone undergoes a two-electron oxidation to quinone (D). The resulting current is directly proportional to the original concentration of the analyte.

Figure 25-19b is a photo of the biosensor array used to carry out the immunoassay described in the previous paragraph. The biosensor consists of an array of electrodes, with each electrode being an independent immunosensor. This arrangement permits multiple proteins to be determined simultaneously. The array was fabricated on glass using photolithographic techniques that are common in the semiconductor industry. In this procedure, the glass substrate was patterned with a polymer (photoresist) that is easily removed by solvent. The pattern of the polymer was the negative of the pattern of the electrodes. Iridium (~100 nm) was then deposited over the entire substrate using sputtering. The polymer was then removed to leave the iridium working and counter electrodes on the substrate. The reference electrode was prepared using a similar procedure and depositing silver. The reference

¹⁹See Figure 33-19 for a photo of a home glucose monitor and Section 33D-3 for a discussion of discrete clinical analyzers.

²⁰For a review of the principles and applications of immunosensors, see P. B. Lippa, L. J. Sokoll, and D. W. Chan, *Clinica Chimica Acta*, **2001**, *314*, 1.

²¹M. S. Wilson and W. Nie, *Anal. Chem.*, **2006**, *78*, 2507.

²²For a discussion of the terms and definitions associated with chemically modified electrodes, see R. A. Durst, A. J. Baumner, R. W. Murray, R. P. Buck, and C. P. Andrieux, *Pure and Applied Chemistry*, **1997**, *69*, 1317. http://www.iupac.org/publications_pac/1997/pdf/6906x1317.pdf.

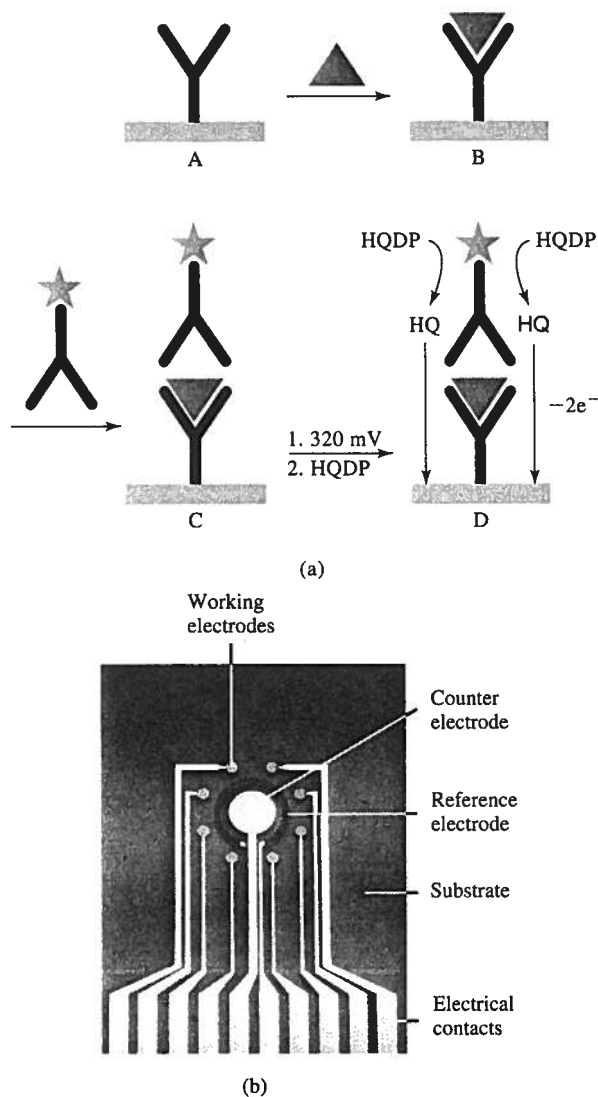


FIGURE 25-19 (a) A: electrode containing immobilized antibody (Y); B: binding of target analyte (\blacktriangledown) to electrode-bound antibody; C: binding of alkaline phosphatase-labeled antibody to electrode-bound analyte; D: application of 320 mV to the electrode and addition of hydroquinone diphosphate (HQDP). Electrochemical oxidation of AP-generated hydroquinone (HQ) generates a current at the electrode that is proportional to the amount of analyte bound to the electrode. (b) Photograph of the biosensor showing the arrangement of IrOx 1-mm-diameter working electrodes, 4-mm-diameter counter electrode, 7-mm-outside-diameter Ag-AgCl reference electrode, and electrical contacts on the substrate ($28 \times 35 \times 1$ mm). For clarity, the sample well is not shown. (Adapted from M. S. Wilson and W. Nie, *Anal. Chem.*, **2006**, *78*, 2507, with permission of the American Chemical Society.) Image reprinted with permission from *Anal. Chem.* Copyright 2006 American Chemical Society.

electrode was then completed by electrochemical deposition of AgCl from a solution containing KCl and added Ag^+ . The array was coated with an insulating polymer film leaving the electrode and contact areas exposed, and finally, a cylindrical polycarbonate well (not shown) was attached over the electrodes to contain the analyte solution.

The 0.785-mm^2 Ir working electrodes were then electrochemically activated to build up a layer of iridium oxide on each. The porous oxide was grown to increase the surface area available for antibody immobilization on the electrode. Drops of solution containing the appropriate antibodies were then applied over the working electrodes, and the array was incubated at 4°C to complete the immobilization.

Analyses were performed on serum samples containing a mixture of goat IgG, mouse IgG, human IgG, and chicken IgY antibodies (0–125 ng/mL). In this assay, the target analytes were also antibodies (IgG and IgY), and so the capture and detection antibodies were antibodies toward antibodies (anti-IgG and anti-IgY). Analyte solutions were added to the sensor well, followed by a mixture of detection antibodies. To perform the electrochemical measurements, the biosensor was connected to a multichannel computer-controlled potentiostat via the edge contacts of the array, and current measurements were made on all eight working electrodes.

The precision of the measurements ranged from 1.9% to 8.2% relative standard deviation, and the detection limit was 3 ng/mL for all analytes. The results compare quite favorably (2.4%–6.5% difference) with results from commercial single-analyte assays using spectroscopic enzyme-linked immunosorbent assays (ELISAs). In this application, four analytes were determined in duplicate, but any combination of up to eight analytes may be determined simultaneously. It is anticipated that when the array biosensor is coupled with a microfluidics system (Section 33C) for solution handling, the combined device will become a powerful tool for the routine determination of this important class of biochemical analytes.

Amperometric Titrations

Hydrodynamic voltammetry can be used to estimate the equivalence point of titrations if at least one of the participants or products of the reaction involved is oxidized or reduced at a working electrode. Here, the current at some fixed potential in the limiting-current region is measured as a function of the reagent volume

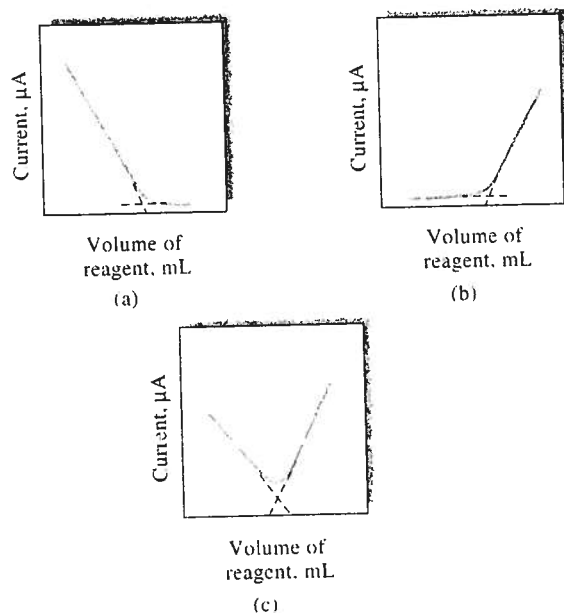


FIGURE 25-20 Typical amperometric titration curves: (a) analyte is reduced, reagent is not; (b) reagent is reduced, analyte is not; (c) both reagent and analyte are reduced.

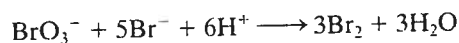
or of time if the reagent is generated by a constant-current coulometric process. Plots of the data on either side of the equivalence point are straight lines with different slopes; the end point is established by extrapolation to the intersection of the lines.²³

Amperometric titration curves typically take one of the forms shown in Figure 25-20. Figure 25-20a represents a titration in which the analyte reacts at the electrode but the reagent does not. Figure 25-20b is typical of a titration in which the reagent reacts at the working electrode and the analyte does not. Figure 25-20c corresponds to a titration in which both the analyte and the titrant react at the working electrode.

There are two types of amperometric electrode systems. One uses a single polarizable electrode coupled to a reference electrode; the other uses a pair of identical solid-state electrodes immersed in a stirred solution. For the first, the working electrode is often a rotating platinum electrode constructed by sealing a platinum wire into the side of a glass tube that is connected to a stirring motor.

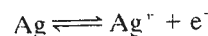
Amperometric titrations with one indicator electrode have, with one notable exception, been confined

to titrations in which a precipitate or a stable complex is the product. Precipitating reagents include silver nitrate for halide ions, lead nitrate for sulfate ion, and several organic reagents, such as 8-hydroxyquinoline, dimethylglyoxime, and cupferron, for various metallic ions that are reducible at working electrodes. Several metal ions have also been determined by titration with standard solutions of ethylenediaminetetraacetic acid (EDTA). The exception just noted involves titrations of organic compounds, such as certain phenols, aromatic amines, and olefins; hydrazine; and arsenic(III) and antimony(III) with bromine. The bromine is often generated coulometrically. It has also been formed by adding a standard solution of potassium bromate to an acidic solution of the analyte that also contains an excess of potassium bromide. Bromine is formed in the acidic medium by the reaction



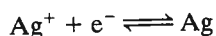
This type of titration has been carried out with a rotating platinum electrode or twin platinum electrodes. There is no current prior to the equivalence point; after the equivalence point, there is a rapid increase in current because of the electrochemical reduction of the excess bromine.

There are two advantages in using a pair of identical metallic electrodes to establish the equivalence point in amperometric titrations: simplicity of equipment and not having to purchase or prepare and maintain a reference electrode. This type of system has been incorporated in instruments designed for routine automatic determination of a single species, usually with a coulometrically generated reagent. An instrument of this type is often used for the automatic determination of chloride in samples of serum, sweat, tissue extracts, pesticides, and food products. The reagent in this system is silver ion coulometrically generated from a silver anode. About 0.1 V is applied between a pair of twin silver electrodes that serve as the indicator system. Short of the equivalence point in the titration of chloride ion, there is essentially no current because no electroactive species is present in the solution. Because of this, there is no electron transfer at the cathode, and the electrode is completely polarized. Note that the anode is not polarized because the reaction



occurs in the presence of a suitable cathodic reactant or depolarizer.

Past the equivalence point, the cathode becomes depolarized because silver ions are present; these ions react to give silver. That is,



This half-reaction and the corresponding oxidation of silver at the anode produce a current whose magnitude is, as in other amperometric methods, directly proportional to the concentration of the excess reagent. Thus, the titration curve is similar to that shown in Figure 25-20b. In the automatic titrator just mentioned, an electronic circuit senses the amperometric detection current signal and shuts off the coulometric generator current. The chloride concentration is then computed from the magnitude of the titration current and the generation time. The instrument has a range of 1 to 999.9 mM Cl^- per liter, a precision of 0.1%, and an accuracy of 0.5%. Typical titration times are about 20 s.

The most common end-point detection method for the Karl Fischer titration for determining water (see Section 24D-1) is the amperometric method with dual polarized electrodes. Several manufacturers offer fully automated instruments for use in performing these titrations. A closely related end-point detection method for Karl Fischer titrations measures the potential difference between two identical electrodes through which a small constant current is passed.

Rotating Electrodes

To carry out theoretical studies of oxidation-reduction reactions, it is often of interest to know how k_A in Equation 25-6 is affected by the hydrodynamics of the system. A common method for obtaining a rigorous description of the hydrodynamic flow of stirred solution is based on measurements made with a rotating disk electrode (RDE), such as the one illustrated in Figure 25-21a and b. When the disk electrode is rotated rapidly, the flow pattern shown by the arrows in the figure is set up. At the surface of the disk, the liquid moves out horizontally from the center of the device, which produces an upward axial flow to replenish the displaced liquid. A rigorous treatment of the hydrodynamics is possible in this case²⁴ and leads to the *Levich equation*²⁵

$$i_l = 0.620 n F A D \omega^{1/2} \nu^{-1/6} c_A \quad (25-15)$$

²⁴A. J. Bard and L. R. Faulkner, *Electrochemical Methods*, 2nd ed., New York: Wiley, 2001, pp. 335–39.

²⁵V. G. Levich, *Acta Physicochimica URSS*, 1942, 17, 257.

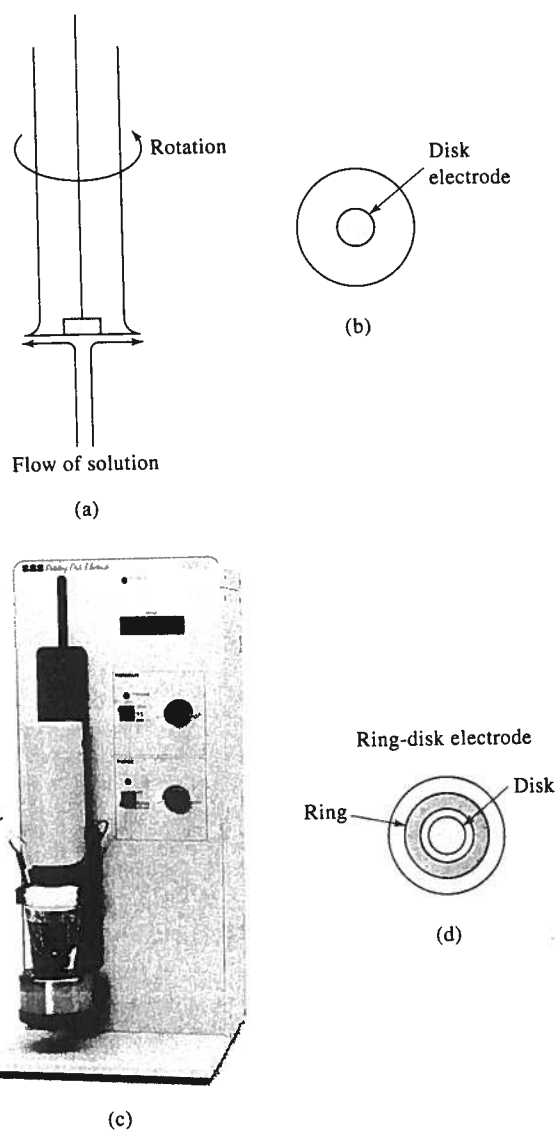


FIGURE 25-21 (a) Side view of an RDE showing solution flow pattern. (b) Bottom view of a disk electrode. (c) Photo of a commercial RDE. (Courtesy of Bioanalytical Systems, Inc., West Lafayette, IN.) (d) Bottom view of a ring-disk electrode.

The terms n , F , A , and D in this equation have the same meaning as in Equation 25-5, ω is the angular velocity of the disk in radians per second, and ν is the *kinematic viscosity* in centimeters squared per second, which is the ratio of the viscosity of the solution to its density. Voltammograms for reversible systems generally have the ideal shape shown in Figure 25-6. Numerous studies of the kinetics and the mechanisms of electrochemical

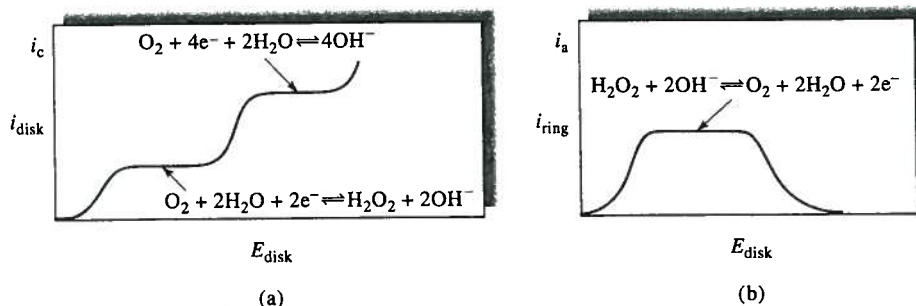


FIGURE 25-22 Disk (a) and ring (b) current for reduction of oxygen at the rotating-ring-disk electrode. (From *Laboratory Techniques in Electroanalytical Chemistry*, 2nd ed., P. T. Kissinger and W. R. Heineman, eds., p. 117, New York: Dekker, 1996. With permission.)

reactions have been performed with RDEs. A common experiment with an RDE is to study the dependence of i_l on $\omega^{1/2}$. A plot of i_l versus $\omega^{1/2}$ is known as a *Levich plot*, and deviations from the linear relationship often indicate kinetic limitations on the electron-transfer process. For example, if i_l becomes independent of ω at large values of $\omega^{1/2}$, the current is not limited by mass transport of the electroactive species to the electrode surface, but instead, the rate of the reaction is the limiting factor. RDEs, such as the versatile commercial model shown in Figure 25-21c, have attracted renewed interest in recent years for both fundamental and quantitative analytical studies as enthusiasm for the dropping mercury electrode (polarography) has faded. RDE detection with a mercury film electrode is sometimes referred to as *pseudopolarography*.

The *rotating-ring-disk electrode* is a modified RDE that is useful for studying electrode reactions; it has little use in analysis. Figure 25-21d shows that a ring-disk electrode contains a second ring-shape electrode that is electrically isolated from the center disk. After an electroactive species is generated at the disk, it is then swept past the ring where it undergoes a second electrochemical reaction. Figure 25-22 shows voltammograms from a typical ring-disk experiment. The curve on the left is the voltammogram for the reduction of oxygen to hydrogen peroxide at the disk electrode. The curve on the right is the *anodic* voltammogram for the oxidation of the hydrogen peroxide as it flows past the ring electrode. Note that when the potential of the disk electrode becomes sufficiently negative so that the reduction product is hydroxide rather than hydrogen peroxide, the current in the ring electrode decreases to zero. Studies of this type provide much useful information about mechanisms and intermediates in electrochemical reactions.

25D CYCLIC VOLTAMMETRY

In *cyclic voltammetry* (CV),²⁶ the current response of a small stationary electrode in an unstirred solution is excited by a triangular voltage waveform, such as that shown in Figure 25-23. In this example, the potential is first varied linearly from +0.8 V to -0.15 V versus an SCE. When the extreme of -0.15 V is reached, the scan direction is reversed, and the potential is returned to its original value of +0.8 V. The scan rate in either direction is 50 mV/s. This excitation cycle is often repeated several times. The voltage extrema at which

²⁶For brief reviews, see P. T. Kissinger and W. R. Heineman, *J. Chem. Educ.*, **1983**, *60*, 702; D. H. Evans, K. M. O'Connell, T. A. Petersen, and M. J. Kelly, *J. Chem. Educ.*, **1983**, *60*, 290.

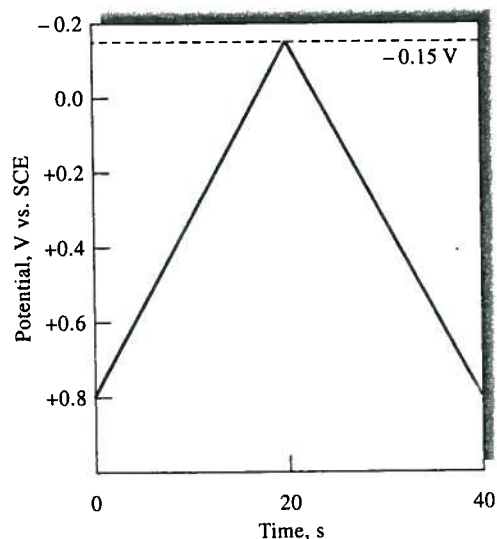
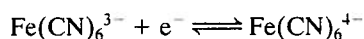


FIGURE 25-23 Cyclic voltammetric excitation signal.

reversal takes place (in this case, -0.15 and $+0.8$ V) are called *switching potentials*. The range of switching potentials chosen for a given experiment is **one in which a diffusion-controlled oxidation or reduction of one or more analytes occurs**. The direction of the initial scan may be either negative, as shown, or positive, depending on the composition of the sample (a scan in the direction of more negative potentials is termed a *forward scan*, and one in the opposite direction is called a *reverse scan*). Generally, cycle times range from 1 ms or less to 100 s or more. In this example, the cycle time is 40 s.

Figure 25-24b shows the current response when a solution that is 6 mM in $\text{K}_3\text{Fe}(\text{CN})_6$ and 1 M in KNO_3 is subjected to the cyclic excitation signal shown in Figures 25-23 and 25-24a. The working electrode was a carefully polished stationary platinum electrode and the reference electrode was an SCE. At the initial potential of $+0.8$ V, a tiny anodic current is observed, which immediately decreases to zero as the scan is continued. This initial negative current arises from the oxidation of water to give oxygen (at more positive potentials, this current rapidly increases and becomes quite large at about $+0.9$ V). No current is observed between a potential of $+0.7$ and $+0.4$ V because no reducible or oxidizable species is present in this potential range. When the potential becomes less positive than approximately $+0.4$ V, a cathodic current begins to develop (point B) because of the reduction of the hexacyanoferrate(III) ion to hexacyanoferrate(II) ion. The reaction at the cathode is then



A rapid increase in the current occurs in the region of B to D as the surface concentration of $\text{Fe}(\text{CN})_6^{3-}$ becomes smaller and smaller. The current at the peak is made up of two components. One is the initial current surge required to adjust the surface concentration of the reactant to its equilibrium concentration as given by the Nernst equation. The second is the normal diffusion-controlled current. The first current then decays rapidly (points D to F) as the diffusion layer is extended farther and farther away from the electrode surface (see also Figure 25-10b). At point F (-0.15 V), the scan direction is switched. The current, however, continues to be cathodic even though the scan is toward more positive potentials because the potentials are still negative enough to cause reduction of $\text{Fe}(\text{CN})_6^{3-}$. As the potential sweeps in the positive direction, eventu-

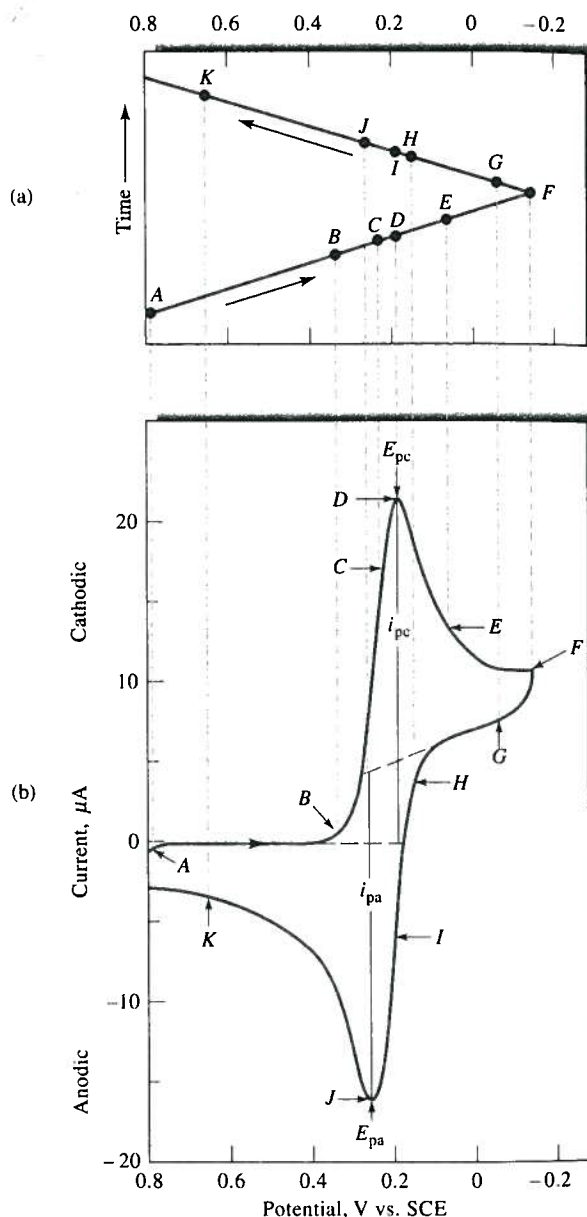


FIGURE 25-24 (a) Potential versus time waveform and (b) cyclic voltammogram for a solution that is 6.0 mM in $\text{K}_3\text{Fe}(\text{CN})_6$ and 1.0 M in KNO_3 . (From P. T. Kissinger and W. H. Heineman, *J. Chem. Educ.*, **1983**, *60*, 702. Copyright 1983; Division of Chemical Education, Inc.)

ally reduction of $\text{Fe}(\text{CN})_6^{3-}$ no longer occurs and the current goes to zero and then becomes anodic. The anodic current results from the reoxidation of $\text{Fe}(\text{CN})_6^{4-}$ that has accumulated near the surface during the forward scan. This anodic current peaks and then decreases as the accumulated $\text{Fe}(\text{CN})_6^{4-}$ is used up by the anodic reaction.



Simulation: Learn more about **cyclic voltammetry**.

Important variables in a cyclic voltammogram are the cathodic peak potential E_{pc} , the anodic peak potential E_{pa} , the cathodic peak current i_{pc} , and the anodic peak current i_{pa} . The definitions and measurements of these parameters are illustrated in Figure 25-24. For a reversible electrode reaction, anodic and cathodic peak currents are approximately equal in absolute value but opposite in sign. For a reversible electrode reaction at 25°C, the difference in peak potentials, ΔE_p , is expected to be

$$\Delta E_p = |E_{pa} - E_{pc}| = 0.0592/n \quad (25-16)$$

where n is the number of electrons involved in the half-reaction. Irreversibility because of slow electron-transfer kinetics results in ΔE_p exceeding the expected value. Although an electron-transfer reaction may appear reversible at a slow sweep rate, increasing the sweep rate may lead to increasing values of ΔE_p , a sure sign of irreversibility. Hence, to detect slow electron-transfer kinetics and to obtain rate constants, ΔE_p is measured for different sweep rates.

Quantitative information is obtained from the Randles-Sevcik equation, which at 25°C is

$$i_p = 2.686 \times 10^5 n^{3/2} A c D^{1/2} \nu^{1/2} \quad (25-17)$$

where i_p is the peak current (A), A is the electrode area (cm^2), D is the diffusion coefficient (cm^2/s), c is the concentration (mol/cm^3), and ν is the scan rate (V/s). CV offers a way of determining diffusion coefficients if the concentration, electrode area, and scan rate are known.

25D-1 Fundamental Studies

The primary use of CV is as a tool for fundamental and diagnostic studies that provides qualitative information about electrochemical processes under various conditions. As an example, consider the cyclic voltammogram for the agricultural insecticide parathion that is shown in Figure 25-25.²⁷ Here, the switching potentials were about -1.2 V and +0.3 V. The initial forward scan was, however, started at 0.0 V and not +0.3 V. Three peaks are observed. The first cathodic peak (A) results from a four-electron reduction of the parathion to give a hydroxylamine derivative

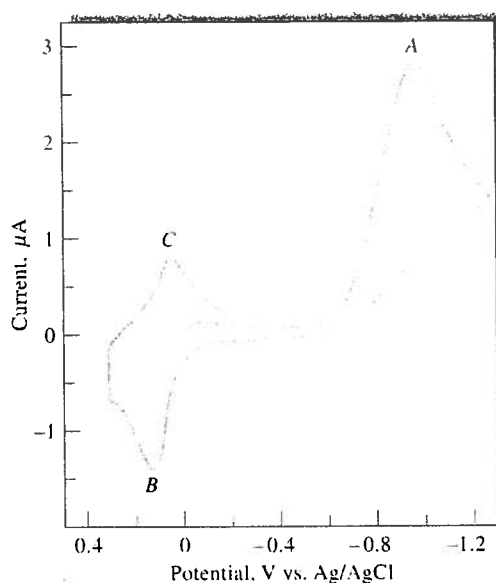
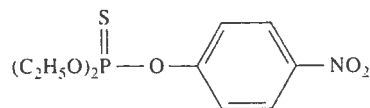
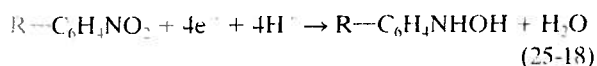
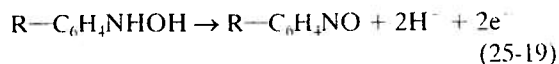
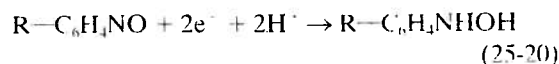


FIGURE 25-25 Cyclic voltammogram of the insecticide parathion in 0.5 M pH 5 sodium acetate buffer in 50% ethanol. Hanging mercury drop electrode. Scan rate: 200 mV/s. (From W. R. Heineman and P. T. Kissinger, *Amer. Lab.*, 1982, no. 11, 34. Copyright 1982 by International Scientific Communications, Inc.)

The anodic peak at B arises from the oxidation of the hydroxylamine to a nitroso derivative during the reverse scan. The electrode reaction is



The cathodic peak at C results from the reduction of the nitroso compound to the hydroxylamine as shown by the equation



Cyclic voltammograms for authentic samples of the two intermediates confirmed the identities of the compounds responsible for peaks B and C.

CV is widely used in organic and inorganic chemistry. It is often the first technique selected for investigation of a system with electroactive species. For example, CV was used to investigate the behavior of the modified electrodes described in Section 25B-2 and shown in Figure 25-5. The resulting cyclic voltammo-

²⁷This discussion and the voltammogram are from W. R. Heineman and P. T. Kissinger, *Amer. Lab.*, 1982 (11), 29.

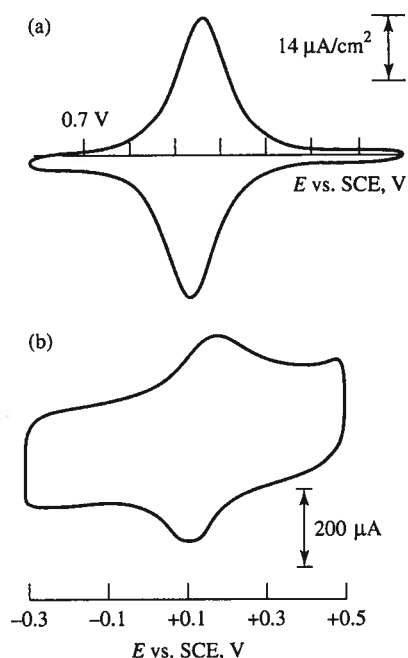


FIGURE 25-26 Cyclic voltammograms of the modified electrodes shown in Figure 25-5. (a) Cyclic voltammogram of a Pt electrode with ferrocene attached. (With permission from J. R. Lenhard and R. W. Murray, *J. Am. Chem. Soc.*, **1978**, *100*, 7870.) In (b), cyclic voltammogram of a graphite electrode with attached $\text{py-Ru}(\text{NH}_3)_5$. (With permission from C. A. Koval and F. C. Anson, *Anal. Chem.*, **1978**, *50*, 223.)

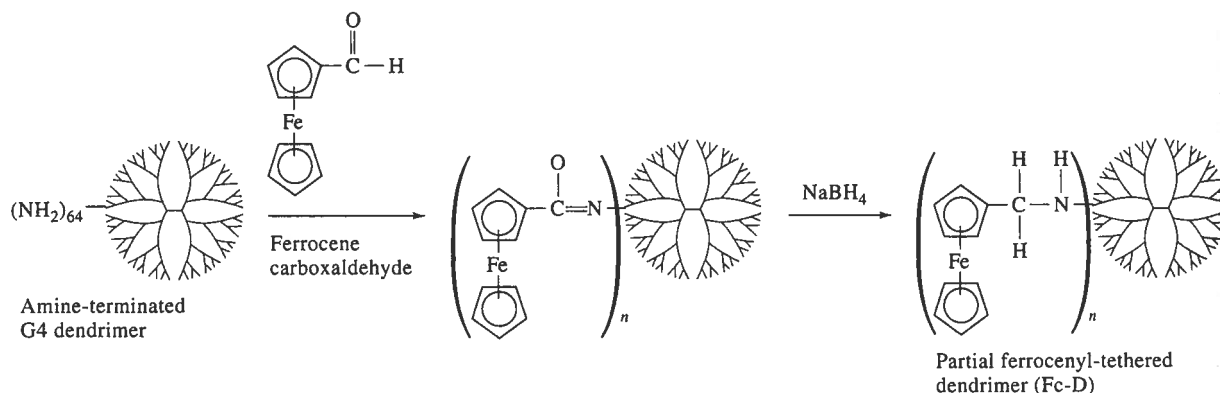
grams shown in Figure 25-26 show the characteristic symmetrical peaks of a reversible surface redox couple. Cyclic voltammograms can reveal the presence of intermediates in oxidation-reduction reactions (for example, see Figure 25-25). Platinum electrodes are often used in CV. For negative potentials, mercury film electrodes can be used. Other popular working electrode

materials include glassy carbon, carbon paste, graphite, gold, diamond, and recently, carbon nanotubes. Chemically modified electrodes, which are discussed in several sections of this chapter, have also been used in CV.

25D-2 Determination of Analytes Using CV

Equation 25-17 shows that peak currents in CV are directly proportional to analyte concentration. Although it is not common to use CV peak currents in routine analytical work, occasionally such applications do appear in the literature, and they are appearing with increasing frequency. As we have mentioned, many modified electrodes are being developed as biosensors. An example is an enzyme-amplified, sandwich-type immunosensor for detecting the interaction between an antigen and an antibody using redox mediation to facilitate electron transfer.²⁸ In this scheme, a self-assembled monolayer is first attached to the surface of a gold electrode to provide a uniform surface with the proper functionality, for attaching subsequent biosensor layers. In the next layer, a ferrocenyl-tethered dendrimer is synthesized as shown in the reaction sequence at the bottom of the page to provide a redox mediator for efficient electron transfer (ferrocene). A *dendrimer* is a spherical polymer molecule that is synthesized in a stepwise fashion to build up onion-like layers of organic functionality. Each successive layer has a larger number of functional sites for binding target molecules.

Approximately 30% of the sixty-four amine groups on the surface of the dendrimer are combined in an imine-formation reaction with the ferrocene carboxaldehyde. Part of the remaining sites are available for binding to the molecular recognition element, which in



²⁸S. J. Kwon, E. Kim, H. Yang, and J. Kwak, *Analyst*, **2006**, *131*, 402.

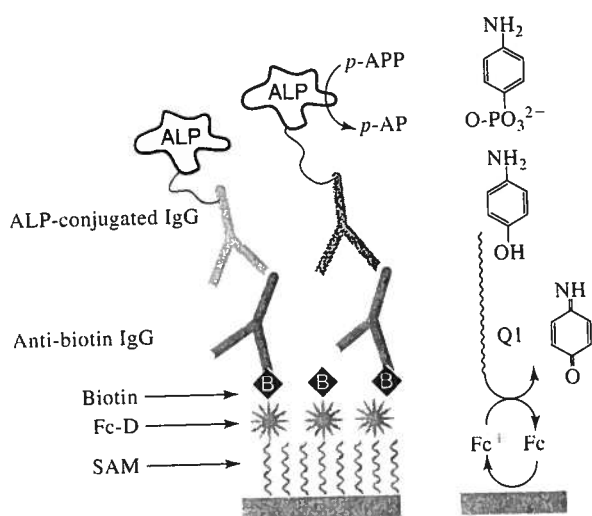


FIGURE 25-27 Schematic illustration of an enzyme-amplified immunosensor using redox mediation of Fc-D. The analyte IgG is shown in blue. (From S. J. Kwon, E. Kim, H. Yang, and J. Kwak, *Analyst*, **2006**, *131*, 402, with permission.)

this example is biotin, on one side of the dendrimer, and part bind to the SAM on the other side.

Figure 25-27 shows how the sandwich arrangement is assembled on the surface of the gold electrode. The SAM layer consists of a 4:1 molar ratio of mercapto-undecanol and mercaptododecanoic acid, so it has on its surface one carboxyl group for every four hydroxyl groups. The ferrocenyl-tethered dendrimer (Fc-D) is then added to the SAM so that a few of the remaining amine groups on the surface of the dendrimer react with carboxyl groups on the SAM to attach the dendrimer to the surface. The final step in the preparation of the working electrode surface is the addition of biotin that is chemically modified with the *N*-hydroxy-succinimide group, with the modified biotin combining with amine groups remaining on the surface of the dendrimer.

In the sandwich immunoassay, the analyte antibody (anti-biotin IgG in the example shown in Figure 25-27) is brought into contact with the working electrode where it binds specifically with the biotin on the surface of the dendrimer. Alkaline phosphatase-conjugated IgG is then added, and it binds specifically with the analyte. The working electrode is then immersed in a buffer containing 1 mM *p*-aminophenylphosphate (*p*-APP) as shown in the figure. This species is converted by alkaline phosphatase to *p*-aminophenol (*p*-AP), which then diffuses to the surface of the dendrimer. Ferrocene (Fc) on the surface of the dendrimer

is oxidized to Fc⁺ when an anodic potential is applied to the working electrode, and Fc⁺ then oxidizes *p*-aminophenol to the quinoid structure Q1 shown in the figure. The magnitude of the resulting current is a measure of the surface concentration of the analyte IgG.

Cyclic voltammograms of working electrodes in the presence of antibodies other than anti-biotin IgG produced no anodic peaks. For analyte solutions containing anti-biotin IgG, CV peak currents were proportional to the concentration of the analyte, and working dose-response curves of CV peak current versus concentration provided an effective means for completing the immunoassay. The detection limit is 0.1 μg/mL, and the range of the technique is 0.1 to 100 μg/mL of anti-biotin IgG.

25D-3 Digital Simulation of Cyclic Voltammograms

Digital simulation of chemical phenomena is a potent tool in fundamental investigations. Over the past four decades, many user-written software applications have appeared in the literature for the simulation of a broad range of electrochemical processes.²⁹ In recent years, investigators and students have benefited from the commercial availability of specialized software packages such as DigiSim.³⁰ This PC-based software uses the fast implicit finite difference method³¹ to simulate cyclic voltammograms for any electrochemical mechanism that can be expressed in terms of single or multiple electron-transfer reactions and to simulate first- and second-order homogeneous chemical reactions. In addition, DigiSim can generate dynamic concentration profiles and display them using a feature called CV—The Movie™. The software can fit simulated data to experimental data that may be imported in a variety of text formats for comparison using least-squares procedures. It can also simulate a range of electrode geometries, finite diffusion, and hydrodynamic mass transport in addition to semi-infinite diffusion.

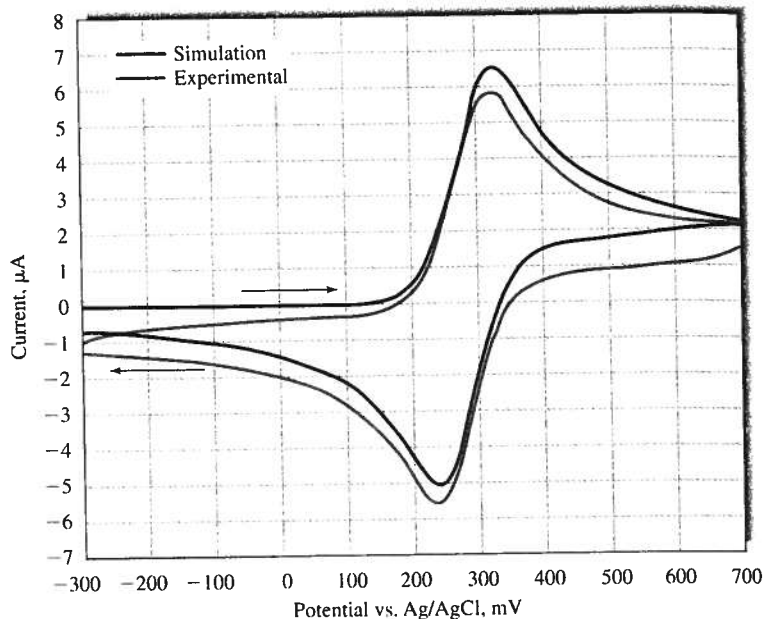
Figure 25-28 shows an experimental cyclic voltammogram of the Fe(CN)₆³⁻-Fe(CN)₆⁴⁻ couple at a boron-doped diamond thin-film electrode compared to a cyclic voltammogram simulated by DigiSim. Note the

²⁹B. Speiser, in *Electroanalytical Chemistry*, A. J. Bard and I. Rubinstein, eds., Vol. 19, New York: Dekker, 1996, pp. 1–108.

³⁰M. Cable and E. T. Smith, *Anal. Chim. Acta.* **2005**, *537*, 299; A. E. Fischer, Y. Show, and G. M. Swain, *Anal. Chem.*, **2004**, *76*, 2553; E. T. Smith, C. A. Davis, and M. J. Barber, *Anal. Biochem.*, **2003**, *323*, 114; for a comprehensive bibliography of principles and applications of DigiSim, see <http://www.epsilon-web.net/Ec/digisim/bibdig.html>.

³¹M. Rudolph, D. P. Reddy, and S. W. Feldberg, *Anal. Chem.*, **1994**, *66*, 589A.

FIGURE 25-28 Experimental and simulated cyclic voltammograms of 0.1 mM $\text{Fe}(\text{CN})_6^{3-}$ - $\text{Fe}(\text{CN})_6^{4-}$ in 1 M KCl at a commercial diamond electrode. (From A. E. Fischer, Y. Show, and G. M. Swain, *Anal. Chem.*, **2004**, 76, 2553 with permission of the American Chemical Society.)



good agreement in the general shape of the two cyclic voltammograms and the excellent correspondence of E_{pc} and E_{pa} . The peak separation $\Delta E_p = E_{pc} - E_{pa}$ can be used to extract the standard heterogeneous rate constant for the electron-transfer process. The two plots are offset because the experimental data contain both faradaic and nonfaradaic (background) contributions to the current, and the simulation represents only the faradaic current.

25E PULSE VOLTAMMETRY

Many of the limitations of traditional linear-scan voltammetry were overcome by the development of pulse methods. We will discuss the two most important pulse techniques, *differential-pulse voltammetry* and *square-wave voltammetry*. The idea behind all pulse-voltammetric methods is to measure the current at a time when the difference between the desired faradaic curve and the interfering charging current is large. These methods are used with many different types of solid electrodes, the HMDE, and rotating electrodes (Section 25C-4).

25E-1 Differential-Pulse Voltammetry

Figure 25-29 shows the two most common excitation signals used in commercial instruments for differential-pulse voltammetry. The first (Figure 25-29a), which is

usually used in analog instruments, is obtained by superimposing a periodic pulse on a linear scan. The second waveform (Figure 25-29b), which is typically used in digital instruments, is the sum of a pulse and a staircase signal. In either case, a small pulse, typically 50-mV, is applied during the last 50 ms of the period of the excitation signal.

As shown in Figure 25-29, two current measurements are made alternately — one (at S1), which is 16.7 ms prior to the dc pulse and one for 16.7 ms (at S2) at the end of the pulse. The difference in current per pulse (Δi) is recorded as a function of the linearly increasing excitation voltage. A differential curve results, consisting of a peak (see Figure 25-30) whose height is directly proportional to concentration. For a reversible reaction, the peak potential is approximately equal to the standard potential for the half-reaction.

One advantage of the derivative-type voltammogram is that individual peak maxima can be observed for substances with half-wave potentials differing by as little as 0.04 to 0.05 V; in contrast, classical and normal-pulse voltammetry require a potential difference of about 0.2 V for resolving waves. More important, however, differential-pulse voltammetry increases the sensitivity of voltammetry. Typically, differential-pulse voltammetry provides well-defined peaks at a concentration level that is 2×10^{-3} that for the classical voltammetric wave. Note also that the current scale for Δi is in nanoamperes. Generally, detection limits with

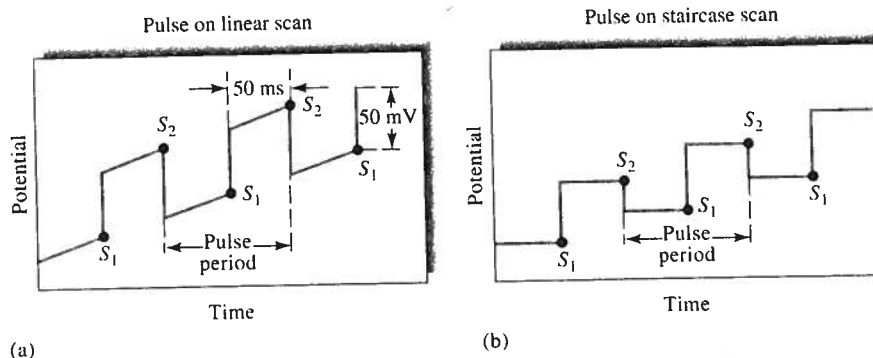


FIGURE 25-29 Excitation signals for differential-pulse voltammetry.

differential-pulse voltammetry are two to three orders of magnitude lower than those for classical voltammetry and lie in the range of 10^{-7} to 10^{-8} M.

The greater sensitivity of differential-pulse voltammetry can be attributed to two sources. The first is an enhancement of the faradaic current, and the second is a decrease in the nonfaradaic charging current. To account for the enhancement, let us consider the events that must occur in the surface layer around an electrode as the potential is suddenly increased by 50 mV. If an electroactive species is present in this layer, there will be a surge of current that lowers the reactant concentration to that demanded by the new potential (see Figure 25-9b). As the equilibrium concentration for that potential is approached, however, the current decays to a level just sufficient to counteract diffusion; that is, to the diffusion-controlled current. In classical voltammetry, the initial surge of current is not observed because the time scale of the measurement is long relative to the lifetime of the momentary current. On the other hand, in pulse voltammetry, the current measurement is made

before the surge has completely decayed. Thus, the current measured contains both a diffusion-controlled component and a component that has to do with reducing the surface layer to the concentration demanded by the Nernst expression; the total current is typically several times larger than the diffusion current. Note that, under hydrodynamic conditions, the solution becomes homogeneous with respect to the analyte by the time the next pulse sequence occurs. Thus, at any given applied voltage, an identical current surge accompanies each voltage pulse.

When the potential pulse is first applied to the electrode, a surge in the nonfaradaic current also occurs as the charge increases. This current, however, decays exponentially with time and approaches zero with time. Thus, by measuring currents at this time only, the nonfaradaic residual current is greatly reduced, and the signal-to-noise ratio is larger. Enhanced sensitivity results.

Reliable instruments for differential-pulse voltammetry are now available commercially at reasonable cost. The method has thus become one of the most widely used analytical voltammetric procedures and is especially useful for determining trace concentrations of heavy metal ions.

25E-2 Square-Wave Voltammetry

Square-wave voltammetry is a type of pulse voltammetry that offers the advantage of great speed and high sensitivity.³² An entire voltammogram is obtained

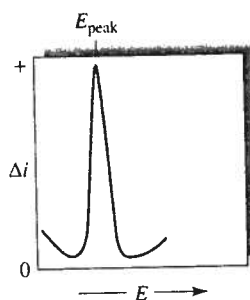


FIGURE 25-30 Voltammogram for a differential-pulse voltammetry experiment. Here, $\Delta i = i_{S_2} - i_{S_1}$ (see Figure 25-29). The peak potential, E_{peak} , is closely related to the voltammetric half-wave potential.

³² For further information on square-wave voltammetry, see A. J. Bard and L. R. Faulkner, *Electrochemical Methods*, 2nd ed., New York: Wiley, 2001, Chap. 7, pp. 293–99; J. G. Osteryoung and R. A. Osteryoung, *Anal. Chem.*, 1985, 57, 101A.

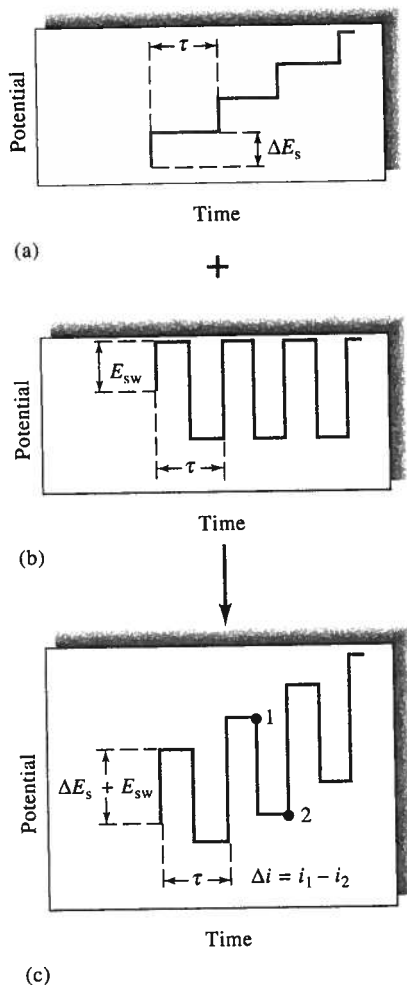


FIGURE 25-31 Generation of a square-wave voltammetry excitation signal. The staircase signal in (a) is added to the pulse train in (b) to give the square-wave excitation signal in (c). The current response Δi is equal to the current at potential 1 minus that at potential 2.

in less than 10 ms. Square-wave voltammetry has been used with HMDEs and with other electrodes (see Figure 25-3) and sensors.

Figure 25-31c shows the excitation signal in square-wave voltammetry, which is obtained by superimposing the pulse train shown in 25-31b onto the staircase signal in 25-31a. The length of each step of the staircase and the period τ of the pulses are identical and usually about 5 ms. The potential step of the staircase ΔE_s is typically 10 mV. The magnitude of the pulse $2E_{sw}$ is often 50 mV. Operating under these conditions, which correspond to a pulse frequency of 200 Hz, a

1-V scan requires 0.5 s. For a reversible reduction reaction, the size of a pulse is great enough so that oxidation of the product formed on the forward pulse occurs during the reverse pulse. Thus, as shown in Figure 25-32, the forward pulse produces a cathodic current i_1 , and the reverse pulse gives an anodic current i_2 . Usually, the difference in these currents Δi is plotted to give voltammograms. This difference is directly proportional to concentration; the potential of the peak corresponds to the voltammetric half-wave potential. Because of the speed of the measurement, it is possible and practical to increase the precision of analyses by signal-averaging data from several voltammetric scans. Detection limits for square-wave voltammetry are reported to be 10^{-7} to 10^{-8} M.

Commercial instruments for square-wave voltammetry are available from several manufacturers, and as a consequence this technique is being used routinely for determining inorganic and organic species. Square-wave voltammetry is also being used in detectors for liquid chromatography.

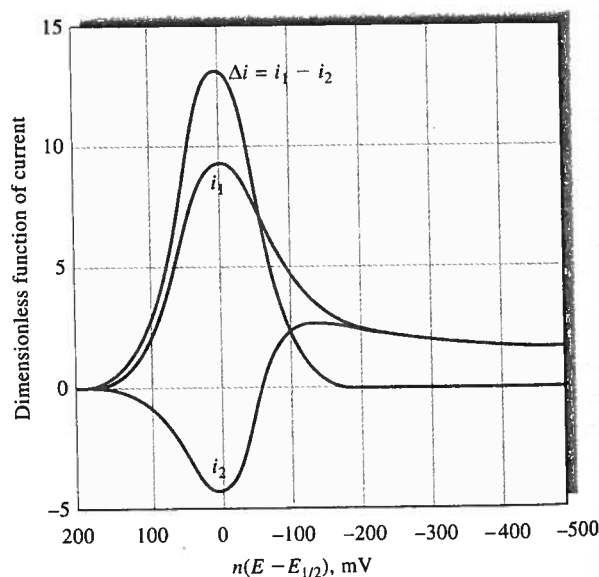


FIGURE 25-32 Current response for a reversible reaction to excitation signal in Figure 25-31c. This theoretical response plots a dimensionless function of current versus a function of potential, $n(E - E_{1/2})$ in millivolts. Here, i_1 = forward current; i_2 = reverse current; $i_1 - i_2$ = current difference. (From J. J. O'Dea, J. Osteryoung, and R. A. Osteryoung, *Anal. Chem.*, **1981**, 53, 695. With permission. Copyright 1981 American Chemical Society.)

25F HIGH-FREQUENCY AND HIGH-SPEED VOLTAMMETRY

As the science, technology, and art of voltammetric instrumentation and data reduction methods have developed, so too have the time and spatial regimes of voltammetry decreased in scale. Traditionally, voltammetric measurements were made at dc and relatively low frequency. As a result, only relatively slow electron-transfer processes could be explored using these methods.

25F-1 Fourier Transform Voltammetry

Just as Fourier transform (FT) methods revolutionized nuclear magnetic resonance and IR spectroscopies, FT methods may have a similar impact on voltammetry. Bond et al.³³ have shown how off-the-shelf PC-based stereo gear coupled with common data-reduction software (MATLAB and LabVIEW) can be used to perform FT voltammetry at sampling frequencies up to 40 kHz. Excitation waveforms of any shape can be synthesized and applied to potentiostatic circuitry, and the resulting response can be analyzed very rapidly to obtain voltammograms corresponding to each of the frequency components of the excitation waveform. The data output from FT voltammetry provides power spectra for each frequency component of the input wave in a new and visually intriguing format. Patterns in the data can be recognized for various types of electron-transfer mechanisms in the chemical systems under study. These workers give several examples, including FT voltammetric measurements on ferrocene and hexacyanoferrate(III), to illustrate the ways that patterns in the output may be analyzed visually. As more and varied systems are explored, databases of mechanisms are cataloged, and software algorithms are applied to recognition of mechanistic patterns, FT voltammetry may become a mainstay in the electrochemical toolkit.

25F-2 Fast-Scan Cyclic Voltammetry

Fast-scan cyclic voltammetry (FSCV) is being extended into biomedical fields, particularly in the areas of neurophysiology and interdisciplinary *psychoanalytical*

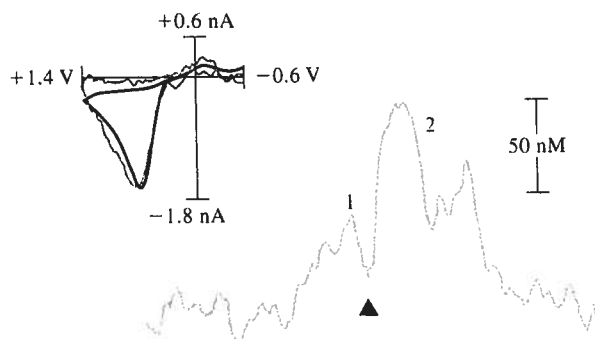


FIGURE 25-33 Dopamine release during cocaine self-administration. Rats were trained to press a lever (arrowhead) to receive a small intravenous injection of cocaine. The lower trace shows changes in dopamine. Peak 1 indicates an increase in dopamine before the rat pressed the lever. The two peaks (2) indicate transients that occurred after the lever press. Underneath the trace, the dark blue bar marks the time the audiovisual cues associated with the lever press were on. The light blue bar indicates when the pump was activated to deliver cocaine. The cyclic voltammogram (black) of behaviorally evoked dopamine matches the electrically evoked voltammogram (blue). (Adapted with permission from P. E. M. Phillips, *Nature*, **2003**, 422, 614.)

electrochemistry. Venton and Wightman have described how FSCV with carbon fiber electrodes can be used to carry out *in vivo* measurements of dopamine release in rat brains during behavioral stimulation.³⁴ In the experiment illustrated by the data in Figure 25-33, a carbon fiber microelectrode (see Section 25I) implanted in the brain of a rat was used as the working electrode as 450-V/s CV scans over +1.4 to -0.6 V were performed at 100-ms intervals. The rat had been previously taught to autoadminister doses of cocaine by pressing a lever.

The two cyclic voltammograms in the upper left of the figure show that dopamine was released both by behavioral stimulation (black trace) and cocaine administration (blue trace). The blue trace in the center shows the concentration of dopamine as a function of time calculated from the peak currents of the voltammograms. The trace was extracted from 200 discrete cyclic voltammograms acquired over the 20-second period shown. The peak at position 1 shows that there

³³A. M. Bond, M. W. Duffy, S. X. Guo, J. Zhang, and D. Elton. *Anal. Chem.*, **2005**, 77, 186A.

³⁴B. J. Venton and R. M. Wightman. *Anal. Chem.*, **2003**, 75, 414A.

was a release of dopamine just prior to the rat autoadministering cocaine as indicated by the black triangle. The peaks at position 2 show a dramatic increase in the release of dopamine as the dosage of cocaine continued, as indicated by the light-blue bar. Studies such as this permit researchers to correlate behavior with chemical changes in the brain.³⁵

25F-3 Nanosecond Voltammetry

To expand frontier knowledge of the electron-transfer process, it is important to be able to conduct CV experiments on a very fast time scale. Careful consideration of the circuit model of Figure 25-7 suggests that the solution resistance and the double-layer capacitance in a voltammetric cell place limitations on the time scale of CV. The time required to charge the double layer is on the order of $R_{\Omega}C_d$, which for a CV cell with a 1-mm-radius Pt electrode immersed in a 1-mM solution of a typical electroactive species might be $500 \Omega \times 0.3 \mu\text{F} = 0.15 \text{ ms}$. Furthermore, the IR drop across the solution resistance in a CV cell carrying a current of 1 mA would be 0.5 V. Acquiring useful CV data at a scan rate of 1000 V/s would be virtually impossible under these conditions. On the other hand, for a 5- μm -radius-disk microelectrode, the IR drop is 2.5 mV and $R_{\Omega}C_d = 750 \text{ ns}$.³⁶ If, in addition to decreasing the size of the working electrode, iterative positive feedback is applied to the excitation waveform,³⁷ the IR drop can be compensated completely, and scan rates of up to 2.5 million V/s can be achieved with properly optimized potentiostatic circuitry. Using such an optimized instrumental setup, cyclic voltammograms of pyrylium cation have been acquired, and kinetics of the dimerization of the reduction product have been measured along with the rate constant of the reaction, which is $k_{\text{dim}} = 0.9(\pm 0.3) \times 10^9 \text{ M/s}$. This value corresponds to a half-life for the pyrylium radical of about 200 ns. The time scale of these measurements is comparable to that of nanosecond flash photolysis experiments. These innovative techniques have opened an entirely new time window for voltammetric measurements, and it is hoped that the goal of observing single-electron-transfer events may be in sight.³⁸

³⁵ P. E. M. Phillips, *Nature*, **2003**, 422, 614.

³⁶ C. Amatore and E. Maisonhaute, *Anal. Chem.*, **2005**, 77, 303A.

³⁷ D. O. Wipf, *Anal. Chem.*, **1996**, 68, 1871.

³⁸ See note 36.

25G APPLICATIONS OF VOLTAMMETRY

In the past, linear-scan voltammetry was used for the quantitative determination of a wide variety of inorganic and organic species, including molecules of biological and biochemical interest. Pulse methods have largely replaced classical voltammetry because of their greater sensitivity, convenience, and selectivity. Generally, quantitative applications are based on calibration curves in which peak heights are plotted as a function of analyte concentration. In some instances the standard-addition method is used in lieu of calibration curves. In either case, it is essential that the composition of standards resemble as closely as possible the composition of the sample, both as to electrolyte concentrations and pH. When this is done, relative precisions and accuracies in the range of 1% to 3% can often be achieved.

25G-1 Inorganic Applications

Voltammetry is applicable to the analysis of many inorganic substances. Most metallic cations, for example, are reduced at common working electrodes. Even the alkali and alkaline-earth metals are reducible, provided the supporting electrolyte does not react at the high potentials required; here, the tetraalkyl ammonium halides are useful electrolytes because of their high reduction potentials.

The successful voltammetric determination of cations frequently depends on the supporting electrolyte that is used. To aid in this selection, tabular compilations of half-wave potential data are available.³⁹ The judicious choice of anion often enhances the selectivity of the method. For example, with potassium chloride as a supporting electrolyte, the waves for iron(III) and copper(II) interfere with one another; in a fluoride medium, however, the half-wave potential of iron(III) is shifted by about -0.5 V and that for copper(II) is altered by only a few hundredths of a volt. The presence of fluoride thus results in the appearance of well-separated waves for the two ions.

Voltammetry is also applicable to the analysis of such inorganic anions as bromate, iodate, dichromate, vanadate, selenite, and nitrite. In general, voltammograms for these substances are affected by the pH of

³⁹ For example, see J. A. Dean, *Analytical Chemistry Handbook*, Section 14, pp. 14.66–14.70, New York: McGraw-Hill, 1995; D. T. Sawyer, A. Sobkowiak, and J. L. Roberts, *Experimental Electrochemistry for Chemists*, 2nd ed., pp. 102–30, New York: Wiley, 1995.

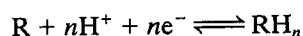
the solution because the hydrogen ion is a participant in their reduction. As a consequence, strong buffering to some fixed pH is necessary to obtain reproducible data (see next section).

25G-2 Organic Voltammetric Analysis

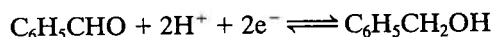
Almost from its inception, voltammetry has been used for the study and determination of organic compounds, with many papers being devoted to this subject. Several organic functional groups are reduced at common working electrodes, thus making possible the determination of a wide variety of organic compounds.⁴⁰ Oxidizable organic functional groups can be studied voltammetrically with platinum, gold, carbon, or various modified electrodes.

Effect of pH on Voltammograms

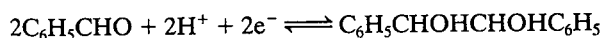
Organic electrode processes often involve hydrogen ions, the typical reaction being represented as



where R and RH_n are the oxidized and reduced forms of the organic molecule. Half-wave potentials for organic compounds are therefore pH dependent. Furthermore, changing the pH may produce a change in the reaction product. For example, when benzaldehyde is reduced in a basic solution, a wave is obtained at about -1.4 V, attributable to the formation of benzyl alcohol:



If the pH is less than 2, however, a wave occurs at about -1.0 V that is just half the size of the foregoing one; here, the reaction involves the production of hydrobenzoin:



At intermediate pH values, two waves are observed, indicating the occurrence of both reactions.

We must emphasize that an electrode process that consumes or produces hydrogen ions will alter the pH of the solution at the electrode surface, often drastically, unless the solution is well buffered. These changes affect the reduction potential of the reaction

and cause drawn-out, poorly defined waves. Moreover, where the electrode process is altered by pH, as in the case of benzaldehyde, the diffusion current-concentration relationship may also be nonlinear. Thus, in organic voltammetry good buffering is generally vital for the generation of reproducible half-wave potentials and diffusion currents.

Solvents for Organic Voltammetry

Solubility considerations frequently dictate the use of solvents other than pure water for organic voltammetry; aqueous mixtures containing varying amounts of such miscible solvents as glycols, dioxane, acetonitrile, alcohols, Cellosolve, or acetic acid have been used. Anhydrous media such as acetic acid, formamide, diethylamine, and ethylene glycol have also been investigated. Supporting electrolytes are often lithium or tetraalkyl ammonium salts.

Reactive Functional Groups

Organic compounds containing any of the following functional groups often produce one or more voltammetric waves.

1. The carbonyl group, including aldehydes, ketones, and quinones, produce voltammetric waves. In general, aldehydes are reduced at lower potentials than ketones; conjugation of the carbonyl double bond also results in lower half-wave potentials.
2. Certain carboxylic acids are reduced voltammetrically, although simple aliphatic and aromatic monocarboxylic acids are not. Dicarboxylic acids such as fumaric, maleic, or phthalic acid, in which the carboxyl groups are conjugated with one another, give characteristic voltammograms; the same is true of certain keto and aldehyde acids.
3. Most peroxides and epoxides yield voltammetric waves.
4. Nitro, nitroso, amine oxide, and azo groups are generally reduced at working electrodes.
5. Most organic halogen groups produce a voltammetric wave, which results from replacement of the halogen group with an atom of hydrogen.
6. The carbon-carbon double bond is reduced when it is conjugated with another double bond, an aromatic ring, or an unsaturated group.
7. Hydroquinones and mercaptans produce anodic waves.

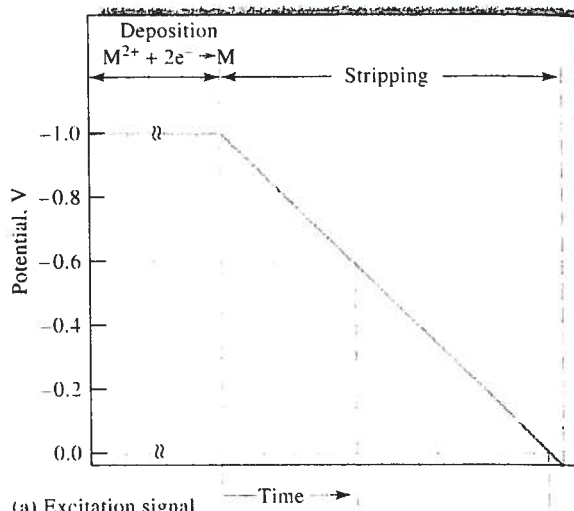
In addition, a number of other organic groups cause catalytic hydrogen waves that can be used for analysis.

⁴⁰For a detailed discussion of organic electrochemistry, see *Encyclopedia of Electrochemistry*, A. J. Bard and M. Stratmann, eds., Vol. 8, *Organic Electrochemistry*, H. J. Schäfer, ed., New York: Wiley, 2002; *Organic Electrochemistry*, 4th ed., H. Lund and O. Hammerich, eds., New York: Dekker, 2001.

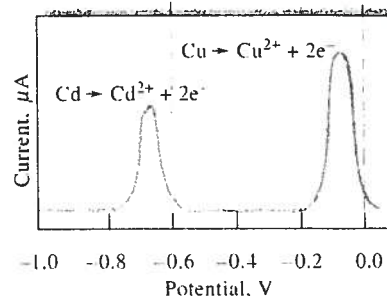
These include amines, mercaptans, acids, and heterocyclic nitrogen compounds. Numerous applications to biological systems have been reported.⁴¹

Stripping methods encompass a variety of electrochemical procedures having a common, characteristic initial step.⁴² In all of these procedures, the analyte is first deposited on a working electrode, usually from a stirred solution. After an accurately measured period, the electrolysis is discontinued, the stirring is stopped, and the deposited analyte is determined by one of the voltammetric procedures that have been described in the previous section. During this second step in the analysis, the analyte is redissolved or stripped from the working electrode; hence the name attached to these methods. In anodic stripping methods, the working electrode behaves as a cathode during the deposition step and as an anode during the stripping step, with the analyte being oxidized back to its original form. In a cathodic stripping method, the working electrode behaves as an anode during the deposition step and as a cathode during stripping. The deposition step amounts to an electrochemical preconcentration of the analyte; that is, the concentration of the analyte in the surface of the working electrode is far greater than it is in the bulk solution. As a result of the preconcentration step, stripping methods yield the lowest detection limits of all voltammetric procedures. For example, anodic stripping with pulse voltammetry can reach nanomolar detection limits for environmentally important species, such as Pb^{2+} , Ca^{2+} , and Tl^+ .

Figure 25-34a illustrates the voltage excitation program that is followed in an anodic stripping method for determining cadmium and copper in an aqueous solution of these ions. A linear scan method is often used to complete the analysis. Initially, a constant cathodic potential of about -1 V is applied to the working electrode, which causes both cadmium and copper ions to be reduced and deposited as metals. The electrode is maintained at this potential for several minutes until a significant amount of the two metals has accumulated



(a) Excitation signal



(b) Voltammogram

FIGURE 25-34 (a) Excitation signal for stripping determination of Cd^{2+} and Cu^{2+} . (b) Stripping voltammogram.

at the electrode. The stirring is then stopped for 30 s or so while the electrode is maintained at -1 V . The potential of the electrode is then decreased linearly to less negative values and the current in the cell is recorded as a function of time, or potential. Figure 25-34b shows the resulting voltammogram. At a potential somewhat more negative than -0.6 V , cadmium starts to be oxidized, causing a sharp increase in the current. As the deposited cadmium is consumed, the current peaks and then decreases to its original level. A second peak for oxidation of the copper is then observed when the potential has decreased to approximately -0.1 V . The heights of the two peaks are proportional to the weights of deposited metal.

Stripping methods are important in trace work because the preconcentration step permits the determination of minute amounts of an analyte with reasonable accuracy. Thus, the analysis of solutions in the range of 10^{-6} to 10^{-9} M becomes feasible by methods that are both simple and rapid.

⁴¹ *Encyclopedia of Electrochemistry*, A. J. Bard and M. Stratmann, eds., Vol. 9, *Bioelectrochemistry*, G. S. Wilson, ed., New York: Wiley, 2002.

⁴² For detailed discussions of stripping methods, see H. D. Dewald, in *Modern Techniques in Electroanalysis*, P. Vanýsek, ed., Chap. 4, p. 151, New York: Wiley-Interscience, 1996; J. Wang, *Stripping Analysis*, Deerfield Beach, FL: VCH, 1985.

25-31.1 Why Hanging Drop Electrode?

Only a fraction of the analyte is usually deposited during the electrodeposition step; hence, quantitative results depend not only on control of electrode potential but also on such factors as electrode size, time of deposition, and stirring rate for both the sample and standard solutions used for calibration.

Working electrodes for stripping methods have been formed from a variety of materials, including mercury, gold, silver, platinum, and carbon in various forms. The most popular electrode is the HMDE shown in Figure 25-3b. RDEs may also be used in stripping analysis.

To carry out the determination of a metal ion by anodic stripping, a fresh hanging drop is formed, stirring is begun, and a potential is applied that is a few tenths of a volt more negative than the half-wave potential for the ion of interest. Deposition is allowed to occur for a carefully measured period that can vary from a minute or less for 10^{-7} M solutions to 30 min or longer for 10^{-9} M solutions. We should reemphasize that these times seldom result in complete removal of the ion. The electrolysis period is determined by the sensitivity of the method ultimately used for completion of the analysis.

25-31.2 How is the Analyte Determined?

The analyte collected in the working electrode can be determined by any of several voltammetric procedures. For example, in a linear anodic scan procedure, as described at the beginning of this section, stirring is discontinued for 30 s or so after stopping the deposition. The voltage is then decreased at a linear fixed rate from its original cathodic value, and the resulting anodic current is recorded as a function of the applied voltage. This linear scan produces a curve of the type shown in Figure 25-34b. Analyses of this type are generally based on calibration with standard solutions of the cations of interest. With reasonable care, analytical precisions of about 2% relative can be obtained.

Most of the other voltammetric procedures described in the previous section have also been applied in the stripping step. The most widely used of these appears to be an anodic differential-pulse technique. Often, narrower peaks are produced by this procedure, which is desirable when mixtures are analyzed. Another method of obtaining narrower peaks is to use a mercury film electrode. Here, a thin mercury film is electrodeposited on an inert electrode such as glassy carbon. Usually, the mercury deposition is carried out

simultaneously with the analyte deposition. Because the average diffusion path length from the film to the solution interface is much shorter than that in a drop of mercury, escape of the analyte is hastened; the consequence is narrower and larger voltammetric peaks, which leads to greater sensitivity and better resolution of mixtures. On the other hand, the hanging drop electrode appears to give more reproducible results, especially at higher analyte concentrations. Thus, for most applications the hanging drop electrode is used. Figure 25-35 is a differential-pulse anodic stripping voltammogram for five cations in a sample of mineralized honey, which had been spiked with 1×10^{-5} M GaCl_3 . The voltammogram demonstrates good resolution and adequate sensitivity for many purposes.

Many other variations of the stripping technique have been developed. For example, a number of cations have been determined by electrodeposition on a platinum cathode. The quantity of electricity required to remove the deposit is then measured coulometrically. Here again, the method is particularly advantageous for trace analyses. Cathodic stripping methods for the halides have also been developed. In these methods, the halide ions are first deposited as mercury(I) salts on a mercury anode. Stripping is then performed by a cathodic current.

25-31.3 Adsorptive Stripping Methods

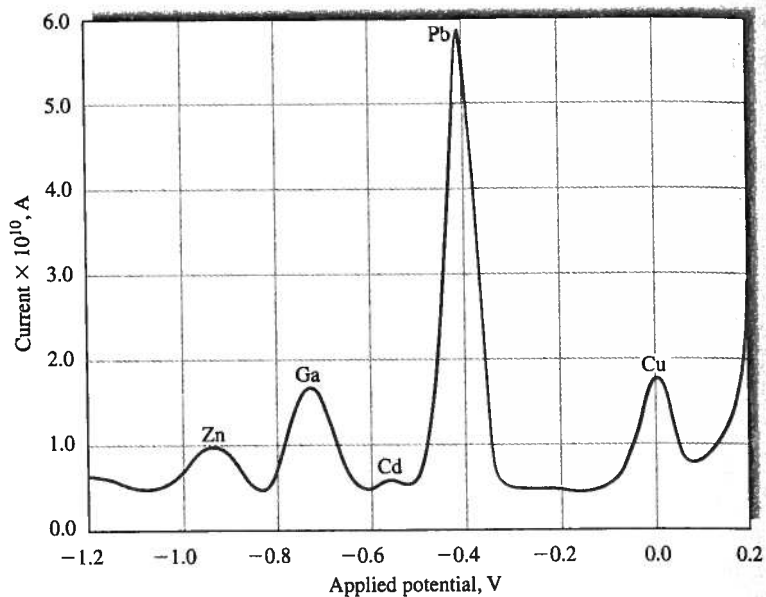
Adsorptive stripping methods are quite similar to the anodic and cathodic stripping methods we have just considered. In this technique, a working electrode is immersed in a stirred solution of the analyte for several minutes. Deposition of the analyte then occurs by physical adsorption on the electrode surface rather than by electrolytic deposition. After sufficient analyte has accumulated, the stirring is discontinued and the deposited material determined by linear scan or pulsed voltammetric measurements. Quantitative information is acquired by calibration with standard solutions that are treated in the same way as samples.

Many organic molecules of clinical and pharmaceutical interest have a strong tendency to be adsorbed from aqueous solutions onto a mercury or carbon surface, particularly if the surface is maintained at a voltage where the charge on the electrode is near zero. With good stirring, adsorption is rapid, and only 1 to 5 min is required to accumulate sufficient analyte for analysis from 10^{-7} M solutions and 10 to 20 min for



Tutorial: Learn more about **stripping methods**.

FIGURE 25-35 Differential-pulse anodic stripping voltammogram in the analysis of a mineralized honey sample spiked with GaCl_3 (final concentration in the analysis solution: 1×10^{-5} M). Deposition potential: -1.20 V; deposition time: 1200 s in unstirred solution; pulse height: 50 mV; and anodic potential scan rate: 5 mVs^{-1} . (Adapted from G. Sanna, M. I. Pilo, P. C. Piu, A. Tapparo, and R. Seeber, *Anal. Chim. Acta*, **2000**, *415*, 165, with permission.)



10^{-9} M solutions. Figure 25-36a illustrates the sensitivity of differential-pulse adsorptive stripping voltammetry when it is applied to the determination of calf-thymus DNA in a 0.5 mg/L solution. Figure 25-36b shows the dependence of the signal on deposition time. Many other examples of this type can be found in the recent literature.

Adsorptive stripping voltammetry has also been applied to the determination of a variety of inorganic cations at very low concentrations. In these applications the cations are generally complexed with surface active complexing agents, such as dimethylglyoxime, catechol, and bipyridine. Detection limits in the range of 10^{-10} to 10^{-11} M have been reported.

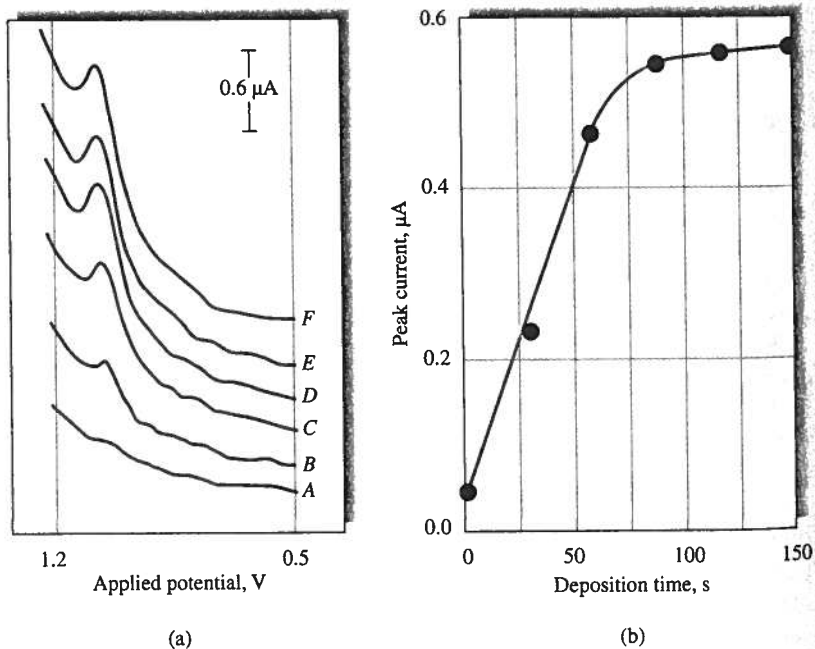


FIGURE 25-36 Effect of preconcentration period on the voltammetric (a) stripping response at the pretreated carbon paste electrode. Preconcentration at $+0.5$ V for (A) 1, (B) 30, (C) 60, (D) 90, (E) 120, and (F) 150 s. Square-wave amplitude, 10 mV; frequency, 40 Hz; 0.5 mg/L calf-thymus DNA. (b) Peak current versus deposition time. (Adapted from J. Wang, X. Cai, C. Jonsson, and M. Balakrishnan, *Electroanalysis*, **1996**, *8*, 20, with permission.)

251 VOLTAMMETRY WITH MICROELECTRODES

In recent years, many voltammetric studies have been carried out with electrodes that have dimensions smaller by an order of magnitude or more than normal working electrodes. The electrochemical behavior of these tiny electrodes is significantly different from classical electrodes and appears to offer advantages in certain analytical applications.⁴³ Such electrodes are often called microscopic electrodes, or *microelectrodes*, to distinguish them from classical electrodes. Figure 25-3c shows one type of commercial microelectrode. The dimensions of these electrodes are typically smaller than about 20 μm and may be as small as 30 nm in diameter and 2 μm long ($A \approx 0.2 \mu\text{m}^2$). Experience has led to an *operational definition of microelectrodes*. A microelectrode is any electrode whose characteristic dimension is, under the given experimental conditions, comparable to or smaller than the diffusion layer thickness, δ . Under these conditions, a steady state or, in the case of cylindrical electrodes, a pseudo-steady state is attained.⁴⁴

251-1 Voltammetric Currents at Microelectrodes

In section 25C-2, we discussed the nature of the current that is produced at an ordinary planar electrode in voltammetric experiments. Using a more elaborate treatment, it can be shown⁴⁵ that the concentration gradient at a spherical electrode following application of a voltage step is

$$\frac{\partial c_A}{\partial x} = c_A^0 \left(\frac{1}{\sqrt{\pi D t}} + \frac{1}{r} \right) = c_A^0 \left(\frac{1}{\delta} + \frac{1}{r} \right) \quad (25-21)$$

where r is the radius of the sphere, $\delta = \sqrt{\pi D t}$ is the thickness of the Nernst diffusion layer, and t is the time after the voltage is applied. Note here that δ is propor-

tional to $t^{1/2}$. By substituting this relation into Equation 25-4, we obtain the time-dependent faradaic current at the spherical electrode.

$$i = nFADc_A^0 \left(\frac{1}{\delta} + \frac{1}{r} \right) \quad (25-22)$$

Note that if $r \gg \delta$, which occurs at short times, the $1/\delta$ term predominates, and Equation 25-22 reduces to an equation analogous to Equation 25-5. If $r \ll \delta$, which occurs at long times, the $1/r$ term predominates, the electron-transfer process reaches a steady state, and the steady-state current then depends only on the size of the electrode. This means that if the size of the electrode is small compared to the thickness of the Nernst diffusion layer, steady state is achieved very rapidly, and a constant current is produced. Because the current is proportional to the area of the electrode, it also means that microelectrodes produce tiny currents. Expressions similar in form to Equation 25-22 may be formulated for other geometries, and they all have in common the characteristic that the smaller the electrode, the more rapidly steady-state current is achieved.

The advantages of microelectrodes may be summarized⁴⁶ as follows:

1. Steady state for faradaic processes is attained very rapidly, often in microseconds to milliseconds. Measurements on this time scale permit the study of intermediates in rapid electrochemical reactions.
2. Because charging current is proportional to the area of the electrode A and faradaic current is proportional to A/r , the relative contribution of charging to the overall current decreases with the size of the microelectrode.
3. Because charging current is minimal with microelectrodes, the potential may be scanned very rapidly.
4. Because currents are so very small (in the picoampere to nanoampere range), the IR drop decreases dramatically as the size of the microelectrode decreases.
5. When microelectrodes operate under steady-state conditions, the signal-to-noise ratio in the current is much higher than is the case under dynamic conditions.
6. The solution at the surface of a microelectrode used in a flow system is replenished constantly, which minimizes δ and thus maximizes faradaic current.
7. Measurements with microelectrodes can be made on incredibly small solution volumes, for example, the volume of a biological cell.

⁴³See R. M. Wightman, *Science*, **1988**, *240*, 415; *Anal. Chem.*, **1981**, *53*, 1325A; S. Pons and M. Fleischmann, *Anal. Chem.*, **1987**, *59*, 1391A; J. Heinze, *Agnew. Chem., Int. Ed.*, **1993**, *32*, 1268; R. M. Wightman and D. O. Wipf, in *Electroanalytical Chemistry*, Volume 15, A. J. Bard, ed., New York: Dekker, 1989; A. C. Michael and R. M. Wightman, in *Laboratory Techniques in Electroanalytical Chemistry*, 2nd ed., P. T. Kissinger and W. R. Heinemann, eds., Chap. 12, New York: Dekker, 1996; C. G. Zoski, in *Modern Techniques in Electroanalysis*, P. Vanýsek, ed., Chap. 6, New York: Wiley, 1996.

⁴⁴For a discussion of microelectrodes, including terminology, characterization, and applications, see K. Stulik, C. Amatore, K. Holub, V. Mareček, and W. Kutner, *Pure Appl. Chem.*, **2000**, *72*, 1483. http://www.iupac.org/publications/pac/2000/7208/7208pdfs/7208stulik_1483.pdf.

⁴⁵See note 43.

⁴⁶See note 43.

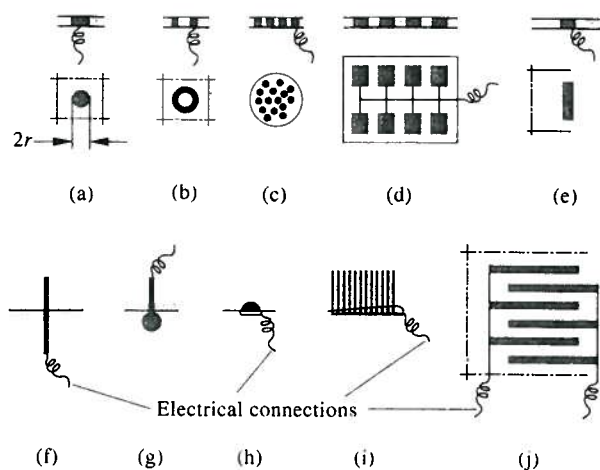


FIGURE 25-37 Most important geometries of microelectrodes and microelectrode arrays: (a) microdisk, (b) microring; (c) microdisk array (a composite electrode); (d) lithographically produced microband array; (e) microband; (f) single fiber (microcylinder); (g) microsphere; (h) microhemisphere; (i) fiber array; (j) interdigitated array. (From K. Štulík, C. Amatore, K. Holub, V. Marek, and W. Kutner, *Pure Appl. Chem.*, **2000**, *72*, 1483, with permission.)

8. Tiny currents make it possible to make voltammetric measurements in high-resistance, nonaqueous solvents, such as those used in normal-phase liquid chromatography.

As shown in Figure 25-37, microelectrodes take several forms. The most common is a planar electrode formed by sealing a 5- μm -radius carbon fiber or a 0.3- to 20- μm gold or platinum wire into a fine capillary tube; the fiber or wires are then cut flush with the ends of the tubes (see Figures 25-3c and 25-37a and b). Cylindrical electrodes are also used in which a small portion of the wire extends from the end of the tube (Figure 25-37f). This geometry has the advantage of larger currents but the disadvantages of being fragile and difficult to clean and polish. Band electrodes (Figure 25-37d and e) are attractive because they can be fabricated on a nanometer scale in one dimension, and their behavior is determined by this dimension except that the magnitude of their currents increases with length. Electrodes of this type of 20 Å have been constructed by sandwiching metal films between glass or epoxy insulators. Other configurations such as the microdisk array, microsphere, microhemisphere, fiber array, and interdigitated array (Figure 25-37c, g, h, i, and

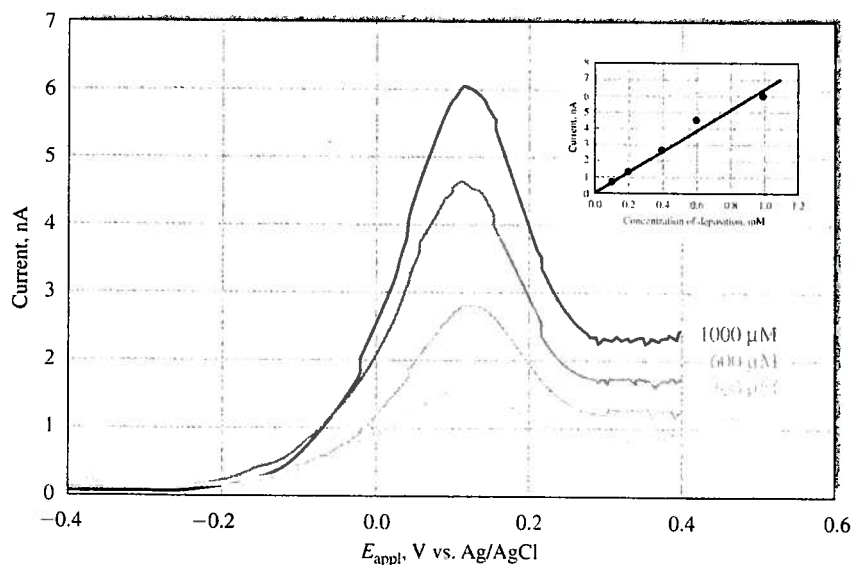


FIGURE 25-38 Detection of dopamine at a multiwall carbon nanotube-based nanoneedle electrode. Differential-pulse voltammograms of dopamine at the nanoneedle electrode in various concentrations from 100 to 1000 μM . Inset is the calibration curve. (From H. Boo et al., *Anal. Chem.*, **2006**, *78*, 617. With permission. Copyright 2006 American Chemical Society.)

j, respectively) have been used successfully. Mercury microelectrodes are formed by electrodeposition of the metal onto carbon or metal electrodes.

25I-2 Applications of Microelectrodes

In Section 25F-2, we described the use of a carbon fiber electrode to monitor concentration of the neurotransmitter dopamine in rat brains in response to behavioral change. In Figure 25-38, we see the results of the differential-pulse voltammetric determination of dopamine at 100–1000 μM levels.⁴⁷ The working electrode in this study was a nanoneedle consisting of a multiwall carbon nanotube attached to the end of a tungsten wire tip. This electrode may be the smallest fabricated up to this time. The entire surface of the probe except the nanoneedle (30 nm in diameter and 3 μm long) was coated with a nonconducting UV-hardening polymer. Both CV and differential-pulse voltammetry were performed with the nanoneedle electrode with good results. The inset in the figure shows a working curve of the peak currents from the voltammograms plotted versus concentration. In light of tremendous interest in nanomaterials and

biosensors for determining analytes in minuscule volumes of solution, it is likely that research and development in this fertile area will continue for some time.

25I-3 The Scanning Electrochemical Microscope

Another application of microelectrodes is the scanning electrochemical microscope (SECM), introduced by Bard in 1989.⁴⁸ The SECM is closely related to the scanning probe microscopes (SPMs) discussed in Section 21G. The SECM works by measuring the current through a microelectrode (the tip) in a solution containing an electroactive species while the tip is scanned over a substrate surface. The presence of the substrate causes a perturbation of the electrochemical response of the tip, which gives information about the characteristics and nature of the surface. Surfaces studied have included solids, such as glasses, polymers, metals, and biological substances, and liquids, such as mercury or oils. The SECM, which is now commercially available, has been used to study conducting polymers, dissolution of crystals, nano materials, and biologically interesting surfaces.

⁴⁷H. Boo et al., *Anal. Chem.*, 2006, 78, 617.

⁴⁸A. J. Bard, F.-R. F. Fan, J. Kwak, and O. Lev, *Anal. Chem.* 1989, 61, 132.

QUESTIONS AND PROBLEMS

*Answers are provided at the end of the book for problems marked with an asterisk.



Problems with this icon are best solved using spreadsheets.

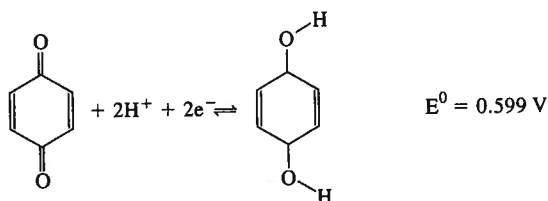
- 25-1** Distinguish between (a) voltammetry and amperometry, (b) linear-scan voltammetry and pulse voltammetry, (c) differential-pulse voltammetry and square-wave voltammetry, (d) an RDE and a ring-disk electrode, (e) faradaic impedance and double-layer capacitance, (f) a limiting current and a diffusion current, (g) laminar flow and turbulent flow, (h) the standard electrode potential and the half-wave potential for a reversible reaction at a working electrode, (i) normal stripping methods and adsorptive stripping methods.
- 25-2** Define (a) voltammograms, (b) hydrodynamic voltammetry, (c) Nernst diffusion layer, (d) mercury film electrode, (e) half-wave potential, and (f) voltammetric sensor.
- 25-3** Why is a high supporting electrolyte concentration used in most electroanalytical procedures?
- 25-4** Why is the reference electrode placed near the working electrode in a three-electrode cell?
- 25-5** Why is it necessary to buffer solutions in organic voltammetry?
- 25-6** Why are stripping methods more sensitive than other voltammetric procedures?

25-7 What is the purpose of the electrodeposition step in stripping analysis?

25-8 List the advantages and disadvantages of the mercury film electrode compared with platinum or carbon electrodes.

25-9 Suggest how Equation 25-13 could be used to determine the number of electrons n involved in a reversible reaction at an electrode.

***25-10** Quinone undergoes a reversible reduction at a voltammetric working electrode. The reaction is



(a) Assume that the diffusion coefficient for quinone and hydroquinone are approximately the same and calculate the approximate half-wave potential (versus SCE) for the reduction of hydroquinone at an RDE from a solution buffered to a pH of 7.0.

(b) Repeat the calculation in (a) for a solution buffered to a pH of 5.0.

***25-11** In experiment 1, a cyclic voltammogram at an HMDE was obtained from a 0.167-mM solution of Pb^{2+} at a scan rate of 2.5 V/s. In experiment 2, a second CV is to be obtained from a 4.38-mM solution of Cd^{2+} using the same HMDE. What must the scan rate be in experiment 2 to record the same peak current in both experiments if the diffusion coefficients of Cd^{2+} and Pb^{2+} are $0.72 \times 10^{-5} \text{ cm}^2 \text{ s}^{-1}$ and $0.98 \text{ cm}^2 \text{ s}^{-1}$, respectively. Assume that the reductions of both cations are reversible at the HMDE.

25-12 The working curve for the determination of dopamine at a nanoneedle electrode by differential-pulse voltammetry (Figure 25-38) was constructed from the following table of data.

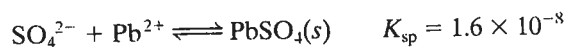
Concentration Dopamine, mM	Peak Current, nA
0.093	0.66
0.194	1.31
0.400	2.64
0.596	4.51
0.991	5.97

- (a) Use Excel to perform a least-squares analysis of the data to determine the slope, intercept, and regression statistics, including the standard deviation about regression.
- (b) Use your results to find the concentration of dopamine in a sample solution that produced a peak current of 3.62 nA. This value is the average of duplicate experiments.
- (c) Calculate the standard deviation of the unknown concentration and its 95% confidence interval assuming that each of the data in the table was obtained in a single experiment.

***25-13** A solution containing Cd^{2+} was analyzed voltammetrically using the standard addition method. Twenty-five milliliters of the deaerated solution, which was 1 M

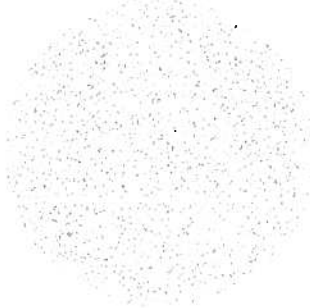
in HNO_3 , produced a net limiting current of $1.78 \mu\text{A}$ at a rotating mercury film working electrode at a potential of -0.85 V (versus SCE). Following addition of 5.00 mL of a $2.25 \times 10^{-3} \text{ M}$ standard Cd^{2+} solution, the resulting solution produced a current of $4.48 \mu\text{A}$. Calculate the concentration of Cd^{2+} in the sample.

- 25-14 Sulfate ion can be determined by an amperometric titration procedure using Pb^{2+} as the titrant. If the potential of a rotating mercury film electrode is adjusted to -1.00 V versus SCE, the current can be used to monitor the Pb^{2+} concentration during the titration. In a calibration experiment, the limiting current, after correction for background and residual currents, was found to be related to the Pb^{2+} concentration by $i_l = 10c_{\text{Pb}^{2+}}$, where i_l is the limiting current in mA and $c_{\text{Pb}^{2+}}$ is the Pb^{2+} concentration in mM. The titration reaction is



If 25 mL of $0.025 \text{ M Na}_2\text{SO}_4$ is titrated with $0.040 \text{ M Pb(NO}_3)_2$, develop the titration curve in spreadsheet format and plot the limiting current versus the volume of titrant.

- 25-15 Suppose that a spherical electrode can be fabricated from a single nano onion, $\text{C}_{60}-\text{C}_{240}-\text{C}_{540}-\text{C}_{960}-\text{C}_{1500}-\text{C}_{2160}-\text{C}_{2940}-\text{C}_{3840}-\text{C}_{4860}$, shown here. Nano onions comprise concentric fullerenes of increasingly larger size as indicated in the formula. Assume that the nano onion has been synthesized with a carbon nanotube tail of sufficient size and strength that it can be electrically connected to a $0.1 \mu\text{m}$ tungsten needle and that the needle and nanotube tail can be properly insulated so that only the surface of the nano onion is exposed.



- Given that the radius of the nano onion is 3.17 nm , find the surface area in cm^2 , neglecting the area of the nanotube attachment.
 - If the diffusion coefficient of analyte A is $8 \times 10^{-10} \text{ m}^2/\text{s}$, calculate the concentration gradient and the current for A at a concentration of 1.00 mM at the following times after the application of a voltage at which A is reduced: $1 \times 10^{-8} \text{ s}$, $1 \times 10^{-7} \text{ s}$, $1 \times 10^{-6} \text{ s}$, $1 \times 10^{-5} \text{ s}$, $1 \times 10^{-4} \text{ s}$, $1 \times 10^{-3} \text{ s}$, $1 \times 10^{-2} \text{ s}$, $1 \times 10^{-1} \text{ s}$, 1 s , and 10 s .
 - Find the steady-state current.
 - Find the time required for the electrode to achieve steady-state current following the application of the voltage step.
 - Repeat these calculations for a $3\text{-}\mu\text{m}$ spherical platinum electrode and for a spherical iridium electrode with a surface area of 0.785 mm^2 .
 - Compare the results for the three electrodes, and discuss any differences that you find.
- 25-16 (a) What are the advantages of performing voltammetry with microelectrodes?
 (b) Is it possible for an electrode to be too small? Explain your answer.

 **Challenge Problem**

25-17 A new method for determining ultrasmall (nL) volumes by anodic stripping voltammetry has been proposed (W. R. Vandaveer and I. Fritsch, *Anal. Chem.*, **2002**, *74*, 3575). In this method, a metal is exhaustively deposited from the small volume to be measured onto an electrode, from which it is later stripped. The solution volume V_s is related to the total charge Q required to strip the metal by

$$V_s = \frac{Q}{nFC}$$

where n is the number of moles of electrons per mole of analyte, F is the faraday, and C is the molar concentration of the metal ion before electrolysis.

- (a) Beginning with Faraday's law (see Equation 22-8), derive the above equation for V_s .
- (b) In one experiment, the metal deposited was Ag(s) from a solution that was 8.00 mM in AgNO₃. The solution was electrolyzed for 30 min at a potential of -0.700 V versus a gold top layer as a pseudoreference. A tubular nano-band electrode was used. The silver was then anodically stripped off the electrode using a linear sweep rate of 0.10 V/s. The following table represents idealized anodic stripping results. By integration, determine the total charge required to strip the silver from the tubular electrode. You can do a manual Simpson's rule integration or do the integration with Excel.⁴⁹ From the charge, determine the volume of the solution from which the silver was deposited.

Potential, V	Current, nA	Potential, V	Current, nA
-0.50	0.000	-0.123	-1.10
-0.45	-0.02	-0.10	-0.80
-0.40	-0.001	-0.115	-1.00
-0.30	-0.10	-0.09	-0.65
-0.25	-0.20	-0.08	-0.52
-0.22	-0.30	-0.065	-0.37
-0.20	-0.44	-0.05	-0.22
-0.18	-0.67	-0.025	-0.12
-0.175	-0.80	0.00	-0.05
-0.168	-1.00	0.05	-0.03
-0.16	-1.18	0.10	-0.02
-0.15	-1.34	0.15	-0.005
-0.135	-1.28	—	—

- (c) Suggest experiments to show whether all the Ag⁺ was reduced to Ag(s) in the deposition step.
- (d) Would it matter if the droplet were not a hemisphere? Why or why not?
- (e) Describe an alternative method against which you might test the proposed method.

⁴⁹S. R. Crouch and F. J. Holler, *Applications of Microsoft® Excel in Analytical Chemistry*, Chap. 11, Belmont, CA: Brooks/Cole, 2004.